Consistently lower sap velocity and growth over nine years of rainfall exclusion in a Mediterranean mixed pine-oak forest

Myriam Moreno, Guillaume Simioni, Maxime Cailleret, Julien Ruffault, Eric Badel, Simon Carrière, Hendrik Davi, Jordane Gavinet, Roland Huc, Jean-Marc Limousin, et al.

Consistently lower sap velocity and growth over nine years of rainfall exclusion in a Mediterranean mixed pine-oak forest

Myriam Moreno[a,b,*], Guillaume Simioni[a], Maxime Cailleret[c], Julien Ruffault[a], Eric Badel[d], Simon Carrière[f], Hendrik Davi[a], Jordane Gavinet[e], Roland Huc[a], Jean-Marc Limousin[e], Olivier Marloie[a], Ludovic Martin[d], Jesús Rodríguez-Calcerrada[g], Michel Vennetier[c], Nicolas Martin-StPaul[a]

[a] INRAE, URFM, Domaine Saint Paul, Centre de recherche PACA, 228 route de l'Aérodrome, CS 40509, Domaine Saint-Paul, Site Agroparc, France.

[b] French Environment and Energy Management Agency 20, avenue du Grésillé- BP 90406 49004 Angers Cedex 01 France.

[c] INRAE, UMR RECOVER, University of Aix-Marseille, 13182 Aix-en-Provence, France.

[d] Université Clermont Auvergne, INRAE, PIAF, F-63000 Clermont-Ferrand, France.

[e] CEFE, Univ Montpellier, CNRS, EPHE, IRD , Univ. Paul Valéry Montpellier 3, Montpellier, France.

[f] Sorbonne Univ., UPMC Univ Paris 06, CNRS, EPHE, UMR 7619 METIS, 4 place Jussieu, 75005 Paris, France.

[g] Departamento de Sistemas y Recursos Naturales, Escuela Técnica Superior de Ingeniería de Montes, Forestal y del Medio Natural, Universidad Politécnica de Madrid. Ciudad Universitaria s/n, 28040, Madrid, Spain.

* Corresponding author:

Email address: myriam.moreno@inrae.fr

Abstract

Mediterranean forests face an intensification of droughts caused by ongoing climate change. To improve our understanding of tree and forest responses to increasing drought, we explored over nine years, the effects of a 30% rainfall exclusion experiment on the water potential, sap velocity and primary and secondary growth of two co-occurring species (*Quercus ilex* and *Pinus halepensis*) in a French Mediterranean forest. In addition, native embolism was measured after six and nine years of exclusion onset. Water potentials decreased earlier during summer drought for both species in the rainfall exclusion plot, and to a higher extent during the drought peak for *Q. ilex*, involving earlier stomatal closure and reduced sap velocity. Sap velocities reduction persisted throughout the years in the exclusion plot. Outside summer the water potential difference between predawn and midday was similar between treatment which indicate that reduced water transport efficiency may be linked to decrease hydraulic conductance. Such differences were neither related to differences in xylem embolism, that remained similar between treatments, nor to change in secondary growth. In contrast primary growth measurements indicate that *P. halepensis* trees, and *Q. ilex* to a lesser extent, experienced reduction in total leaf areas in response to the rainfall exclusion. Globally, our results suggest that increase drought lead, for both species, to a decrease in sap velocity not mediated by increase embolism but rather by a reduction in primary growth. So far little conclusion can be drawn regarding the competitive advantage of one species over the other in the context of increasing drought related to climate change.

Keywords:

Throughfall exclusion, acclimation, embolism, plant hydraulics, diversity, electrical resistivity tomography.

1. Introduction

Forests cover almost a third of the world's land surface and are involved in most biogeochemical processes, the water cycle and the earth's energy balance. In particular, forest trees constitute a net carbon sink and thus act as a buffer against the anthropogenic accumulation of CO_2 in the atmosphere, storing about 25 % of annual global CO_2 emissions (Friedlingstein et al., 2019). However, global warming has already altered and will continue to affect how forests function, in particular because of the increased frequency and severity of droughts in many regions of the world (Dai, 2012). This effect could be especially strong in the Mediterranean basin, which has been identified as a potential "climate change hotspot" (Diffenbaugh & Giorgi, 2012), due to larger increases in temperature (Cramer et al., 2018) and larger decreases in rainfall compared with the global mean, especially during the summer (Lionello & Scarascia, 2018). Mediterranean forests are thus at the forefront of climate changes (FAO and Plan Bleu, 2018) and constitute a key natural laboratory to explore future effects of drought on forest and tree functions.

During a drought, soil and tree water potentials drop because of soil water depletion, which leads to a cascade of physiological reactions (Breda et al., 2006; Choat et al., 2018; McDowell, 2011). Growth decreases rapidly as a result of reduced turgor and meristem activity at relatively high water potential (Lempereur et al., 2015; Muller et al., 2011). Stomata closure then limits the transpiration rate, and thereby the plant water potential decline, but at the detriment of photosynthetic activity (Flexas et al., 2004). If the drought is prolonged and increases in intensity, two phenomena can occur that alter plant function and impair plant vitality (N. McDowell et al., 2008; Nathan G. McDowell, 2011). First, an imbalance between the supply and demand of non-structural carbohydrates can lead to "carbon starvation", leaving the plant unable to maintain its metabolism and/or to defend

against pathogens. Second, a catastrophically low water potential can trigger "hydraulic failure", leading to xylem embolism followed by tissue desiccation and ultimately plant death (Adams et al., 2017; N. Martin-StPaul et al., 2017). However, in spite of the relevance of these processes in drought induced tree death, this simplified view has emerged mainly from short-term greenhouse experiments on seedlings and saplings that are difficult to transfer to more complex, heterogeneous natural conditions and longer timescales (Kawaletz et al., 2014). For instance, a tree's ontogenetic development, size, and drought acclimation history can modify its drought sensitivity over the long run (e.g., Martín-Benito et al., 2008). In addition, the differential drought responses of co-occurring species to multi-year drought and disturbances, may lead to progressive changes in forest succession and dynamic (Nate G. McDowell et al., 2020).

An approach to explore long term changes is via gradient studies, in which time is substituted by space (Klein et al., 2013; Martin-Stpaul et al., 2012). However confounding factors (e.g., differences in soil properties or in stand structure and density between sites) can make comparisons difficult. Retrospective approaches based on tree-ring width or isotopes can also be used to explore long-term drought responses (Gessler et al., 2018; Pellizzari et al., 2016; Timofeeva et al., 2017), but the dependence of these metrics on several physiological mechanisms precludes a comprehensive view of tree drought responses. In addition, some external drivers of tree responses to drought, such as stand composition and density, are hard to trace back and may bias the results of retrospective studies. Rainfall exclusion experiments overcome some of the limitations of the gradient and retrospective studies and are a valuable approach to study long-term drought responses (Beier et al., 2012; Benson et al., 2019; Song et al., 2019)

Several plot-scale rainfall exclusion experiments have been conducted since the 2000s, with most reporting a decrease in tree productivity (Wu et al., 2011). However, not all species

respond in the same way to drought intensification. For example, Ogaya and Penuelas (2007) found that *Arbutus unedo* and *Quercus ilex* had lower stem diameter growth after a five-year 30% reduction in precipitation, but that *Phillyrea latifolia* did not. Moreover, the same species can also respond differently to water stress depending on the site and the experiment duration. Contrary to the previous study, Rodríguez-Calcerrada et al. (2011) did not find any reduction in the radial increment of *Q. ilex* trees when these were subjected to a 27% reduction in rainfall for six years, although they did observe a significant reduction in the crown leaf area. Such species-, time- and site-specific responses highlight the need to monitor rainfall exclusion effects on primary and secondary growth over long periods, and in co-occurring species in different field experiments.

Rainfall exclusion systems used to experimentally increase drought have been found to consistently alter plant water function. Trees exposed to rainfall reduction for more than a year have shown reductions in sap flux ranging from 10 to 60% depending on the amount of rainfall excluded (Fisher et al., 2007; Grossiord et al., 2018; Grossiord, Sevanto, Adams, et al., 2017; Köhler et al., 2010; Limousin et al., 2009; Ward et al., 2015; Wullschleger & Hanson, 2006; Zhang et al., 2018). Interestingly, transpiration reduction in rainfall exclusion experiments tends to persist, even during well-watered periods. This persistent alteration of tree transpiration may result from the combination of several mechanisms operating on different timescales (Martin-StPaul et al., 2013). These include short-term stomatal regulation of transpiration related to earlier summer water stress in drought treatments (Borghetti et al., 1998), and modifications in the tree hydraulic system, which limit water transport on the longer term, for example via a reduction in whole-tree hydraulic conductance (Limousin et al., 2009; Pangle et al., 2015). These changes can be accompanied by changes in the leaf area and the leaf to sapwood area ratio (Hudson et al., 2017).

In this study, we explored how long-term partial (30%) rainfall exclusion affects water stress, growth and water transport in *Pinus halepensis* and *Quercus ilex*, two species that co-occur in the mature mixed Mediterranean forest of Font-Blanche in France. These two forest species are among the most drought-tolerant forest trees in Europe and dominate Mediterranean forests (Delzon et al., 2010; Lobo et al., 2018). They often co-occur in post-disturbed forests such as our study site, following a wildfire for instance. In such cases, seeder *P. halepensis* trees form an upper canopy below which an understory of *Q. ilex* trees develops. *P. halepensis* and *Q. ilex* react differently to drought, the former being more water-saving (isohydric) than the latter, which is more anisohydric, with less tight transpiration control (Baquedano & Castillo, 2006).

Based on measurements of sap velocity, leaf water potential, native xylem embolism, plant area index, and primary and secondary growth (basal area increment and sapwood area estimated through Electrical resistivity tomography measurements on trunks) carried out for nine years, we tested how the two species would be affected by longer and more intense summer droughts, which would be reflected by (i) a more negative water potential compared with control conditions (with *Q. ilex* experiencing lower water potentials than *P. halepensis*, because of the latter's tighter regulation of transpiration and water potential); (ii) reduced sap velocities in response to earlier stomatal closure; (iii) reduced sap velocities in response to reduced tree hydraulic conductance, because of increased summer cavitation and/or long-term adjustments (i.e. a reduced leaf to sapwood area ratio); and (iv) reduced primary and secondary growth and a lower overall stand leaf area index.

2. Materials and methods

2.1. Study site

The Font-Blanche long-term experimental monitoring site is located in a mixed Mediterranean forest in south-eastern France (43°14'27''N, 5°40'45''E; altitude 425 m above sea level) ca. 20 km east of Marseille (Fig. 1a). The experimental area covers 7650 m² and is dominated by *P. halepensis* in the upper tree stratum (average height, 13 m) and *Q. ilex* in the intermediate tree stratum (average height, 5 m). The understorey is composed mainly of five species that do not exceed 4 m in height: *Phillyrea angustifolia*, *Quercus pubescens*, *Quercus coccifera*, *Arbutus unedo* and *Pistacia therebinthus*. The climate is Mediterranean with hot, dry summers. The mean annual temperature and cumulative precipitation over the study period were 14°C and 701 mm, respectively, between 2008 and 2017. The bedrock is karstified Cretaceous limestone with urgonian facies including rudists. The soil is a typical thin and rocky rendzina with a maximum depth of around 50 cm, and a volumetric rock fraction of about 50% at the top, and up to 90% at the bottom. Font-Blanche is part of the Integrated Carbon Observation System (ICOS) and the Analysis and Experiments on Ecosystems (AnaEE-France) networks. The site is equipped with a 17 m eddy-covariance flux tower on top of which meteorological variables (including radiation, rainfall, temperature, vapour pressure deficit), and carbon, water and energy fluxes are continuously monitored at 30 min intervals. Since January 2009, temperature and air relative humidity have been monitored with an HMP45C probe (Vaisala) and precipitation with an automatic rain gauge (R 3029 0.5 mm tipping bucket, Précis Mécanique). In July 2013, more precise sensors were installed for air humidity and temperature (Vaisala HMP155), and rainfall (R 3029 0.2 mm tipping bucket, Précis Mécanique). The soil water content estimated with automatic soil

moisture probes (Decagon EC-5 Volumetric Water Content sensors) within the first 50 cm of soil averages 50 mm (Fig. 1e), while the total soil water available for plants estimated from eddy covariance fluxes average 160 mm. The stone-free fine fraction of the soil is a homogeneous silty clay loam that contains around a third of the available water capacity. The remaining extractable water is located in the bedrock, within fractures and clay pockets.

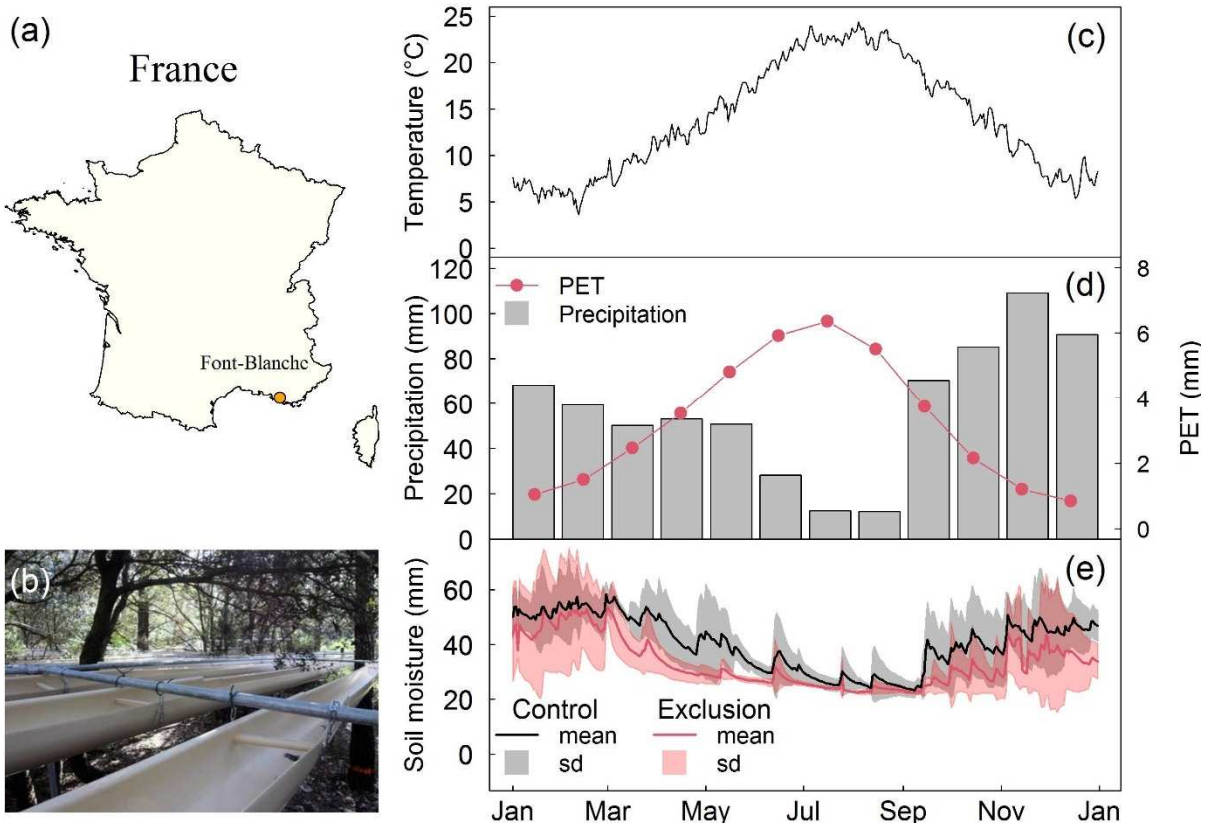

Fig. 1. Description of the Font-blanche site. (a) geographical location. (b) gutters used for rainfall exclusion. (c) mean daily temperature between 2008 and 2017. (d) mean monthly rainfall and potential evapotranspiration (PET) between 2008 and 2017 and (e) Mean and standard deviation of daily soil moisture measured with automatic soil moisture probes at depths of 5–50 cm in the control and rainfall exclusion plots between 2013 and 2017.

In December 2008, a single rainfall exclusion plot was set up, covering an area of 25 × 25 m. It was effective in January 2009 (Fig. 1b). Parallel PVC gutters were hung with a slight

slope approximately 2 m above the ground to cover ~30% of the ground area and thus reduce the precipitation reaching the ground by approximately 30%. Two control plots with the same surface area were also established at the same time. One was equipped with the same gutters as in the rainfall exclusion plot but hung upside down so as not to intercept rainfall. This was done to account for the potential effects of the gutters on the ecosystem albedo and understorey microclimate conditions. The other control plot was left without gutters (the characteristics of the plots are listed in Table S1). Statistical analysis showed no significant difference between the two control plots in terms of sap velocity, water potentials, or stem diameter increments, so the corresponding data were grouped together as a single control treatment. To minimize border and spatial effects and maximize the rainfall exclusion effects, monitored trees were selected in small area within each plot and in the centre of the plot for the exclusion treatment.

2.2. Soil moisture

From 2008 to 2013, soil moisture was monitored every two weeks using time domain reflectometry probes (Moisture.Point model MP-917). Five sensors positioned at soil depths ranging from 5 to 55 cm were installed in each plot. In 2013, four additional soil profiles (three in the control treatment plots and one in the rainfall exclusion plot) were monitored at half-hour intervals using automatic probes (Decagon's EC-5 Volumetric Water Content sensor). The four new profiles consisted of measurements from five sensors positioned at 5 to 50 cm depth. In each sampled layers of the corresponding soil pits, the stones were separated from the soil and immersed in water in a container. Stone volume was estimated using the variation of the water level. The total volume for that layer was measured by measuring the amount of water needed to fill a waterproof bag lining the pit. Sones and soil were put back in the pit, respecting the layer order. The volumetric water content measured by each sensor was

converted to millimetres after accounting for the proportion of stones in the corresponding soil layer.

Given the high soil heterogeneity, the limited number of probes may not be sufficient to yield representative soil moisture. Additionally, these measurements do not cover the full depth explored by the roots. Actually, two thirds of the water holding capacity being contained deeper under the bedrock. We thus used additional simulations of soil moisture dynamic under control and exclusion treatment by using the forest stand water balance model Biljou© (Granier et al., 1999). This model computes the different component of the water balance at a daily time scale using a set of meteorological data (wind speed, relative humidity, precipitation, radiation and temperature) as well as soil and stand characteristics (number of layer and their soil bulk density, maximum extractable water and wilting point by layer, Maximum LAI). All these required parameters were measured on the site (Table S2). Simulations were made for both treatments. For the rainfall exclusion treatment, the daily precipitation was reduced by 30% and the rest of the parameters, except LAI, were kept constant. The relative extractable water calculated by the model was used in the study to represent soil water dynamic in each treatment. The online platform was used to perform the simulations (https://appgeodb.nancy.inra.fr/biljou/).

Strong relationships were found between predicted relative extractable water (REW) and predawn water potential (Ψpd) (Fig. S1, $R^2 = 0.8$ for both species) giving confidence that the model is relevant for estimating and comparing the available water of both treatments.

2.3*. Plant area index*

Plant area index was regularly monitored using hemispherical photographs taken every one to two months. For the present study, we used only data taken during summer, at the peak of foliage growth. Photos were taken at eight locations in each plot, roughly following a

228 regular 5 × 5 meters grid (i.e. the distance between photos could vary between 7 and 10 m
229 depending on the presence of stumps that precluded the installation of the camera). From
230 2008 to 2015, we used a Canon 5D camera equipped with a sigma 8 mm EX DG fisheye lens,
231 and from 2015 to 2018 a Nikon D3200 camera with a sigma 4.5 mm EX DC HSM fisheye
232 lens. The camera was positioned skywards and oriented so that the north would be at the top
233 of the picture. The camera was mounted 2 m above the ground on a self-levelling platform
234 (manufactured at INRAE-URFM, Avignon, France), to avoid any influence of the gutters or
235 of understorey vegetation. Unusually tall understorey plants proved nonetheless to be a
236 problem in some locations, and these were excluded from the analysis. The analysed data
237 come from 6 locations in the rainfall exclusion plot and 12 locations in the control plots.
238 Photos were taken when the sun was low (mostly at sunset) or, very rarely, when the sky was
239 uniformly overcast. They were taken in RAW format, and later converted with the software
240 DCRAW with no gamma correction. The images were processed and analysed using a set of
241 macros written for the ImageJ software (Schneider et al., 2012): extraction of the blue
242 channel, automatic contrast adjustment, manual double thresholding, and calculation of the
243 gap fraction and of the plant area index (PAI). Thresholding was carried out as described by
244 Leblanc et al. (2005) and the PAI was calculated using Miller's formula, as approximated by
245 Welles and Norman (1991).

246 ***2.4.*** *Primary growth*

247 Primary branch growth was monitored monthly from 2008 to 2010 for *Q. ilex*, and from
248 2008 to 2017 for *P. halepensis*. For *Q. ilex*, measurements were made on 9 and 12 trees in the
249 exclusion and control plots, respectively (on 38 and 62 branches, respectively). Branches were
250 analysed at two heights in the canopy (bottom and top canopy branches). Measurements
251 included the number of ramifications and the shoot length.

For *P. halepensis*, measurements were performed on 4 trees in the exclusion plot and on 7 trees in the control plot. In total, 481 branches of different vigour (assessed from annual shoot length) (Girard et al., 2012), different architectural order (second and third), and from different locations in the canopy (bottom, middle and top of the crown) were chosen to span the range of possible growth rates within a tree. For each branch, we measured (i) the annual shoot length, which is a good proxy for the number of needles carried by the shoot once the presence of male flowers was accounted for (Fig. A1); (ii) the annual branching rate (i.e. the number of branches per shoot length); and (iii) the mean annual needle length. As *P. halepensis* is highly polycyclic (Girard et al., 2012), the annual needle length was calculated by averaging the needle length of the different growth units weighted by the length of the respective unit. On these branches, we also retrospectively calculated annual shoot lengths and branching rates as far back as 2000 based on morphological markers, such as the size and density of scales at the base of the growth units (Pardos et al., 2003).

2.5. Secondary growth

2.5.1. Basal area increment

Tree stem circumferences at breast height were measured in the rainfall exclusion and control plots in 2007, 2009, and annually from 2011 onwards. However, because of the low growth rates, especially of *Q. ilex*, we aggregated annual circumference increments over the entire period since the start of rainfall exclusion (i.e. from 2009 to 2017) and converted them into basal area increment (BAIs). To limit edge effects resulting from tree roots extending outside the rainfall exclusion area, trees located less than 5 m from the border of the rainfall exclusion plot were excluded from the analysis.

2.5.2 Sapwood area /basal area ratio based on Electrical Resistivity Tomography of tree trunk.

Fifteen (7 *P. halepensis*, 8 *Q. ilex*) and ten (5 *P. halepensis*, 5 *Q. ilex*) healthy trees were selected from the control and the rainfall exclusion plots respectively. Electrical resistivity tomography (ERT) was performed using a commercial multichannel, multielectrode resistivity system (PICUS TreeTronic 3, Argus Electronic gmbh, Rostock, Germany) during February 2020. For each tree, depending on their circumference, between 8 and 24 nail probes were hammered at breast height (130 cm) equally distributed around the trunk until they reached the sapwood of the xylem. Nails were inserted counterclockwise and starting with a northward orientation. Exact positions of nail probes and trees geometry were measured using an electronic calliper (PICUS Calliper Version 3, Argus Electronic Gmbh) connected via Bluetooth to the PICUS Treetronic 3 tomograph. For each ERT measurement, nail probes were connected via electrodes to the resistivity system. The system automatically determined the appropriate electric voltages to apply between all MPs, measured the intensity and deduced the mean resistivity between the nails. Then, all data (geometry and ERT) were sent to the TreeTronic expert software Q74 (Argus Electronic Gmbh) on a laptop for a 2D

290 reconstruction step. The R script provided by Benson et al. (2019) under the supplementary
291 material was then used to build electrical resistivity tomographs (Fig. S2-S3) with a colour
292 scale ranging from blue (low resistivity) to red (high resistivity) and calculate sapwood depth
293 and area, considering that the heartwood-sapwood boundary is characterized by a threshold
294 resistivity value. This value is identified by the algorithm as the steepest change in resistivity
295 with depth in radials profiles (Guyot et al., 2013). To cross-validate sapwood estimation from
296 the algorithm, we compared resistivity profile with water content profiles for one *P.*
297 *halepensis* and one *Q. ilex* sampled outside the plots area. One sample for each of the two
298 trees were taken at DBH hight after ERT profiles were measured. Water content profile (per
299 unit dry mass) was measured at a 1cm resolution on the core. The comparison of water
300 content and resistivity profiles indicate that the decline in water content match closely the
301 increase in resistivity (Fig. S4).

302 ***2.6****. Tree water potential*

303 Predawn and midday water potentials were measured every summer season from 2008 to
304 2017. Measurement dates varied between years from three to six field campaigns depending
305 on drought duration. They were always performed on days with clear sky and little wind.
306 Measurements were made on twigs from 4 to 6 trees per species and per plot using a
307 Scholander pressure chamber (manufactured at INRAE, Avignon, France). Trees were chosen
308 so as to cover the range of sizes present in each plot. To limit edge effects derived from roots
309 of border trees extending outside the rainfall exclusion area, only trees located more than 5 m
310 from the border of the rainfall exclusion plot were selected. Midday water potentials were
311 measured on well-lit, sun-exposed shoots. Samples were collected between midday and 2 pm
312 for midday potentials, and during the two hours preceding sunrise for predawn potentials.
313 Measurements were made on-site. Generally, one sample was measured per tree. In the very

few cases when a difference of more than 1 MPa was observed between trees in the same plot, additional measurements were performed on the tree(s) with suspicious value(s). Sap flow driving force ($\Delta\Psi$) was calculated as the difference between predawn and midday water potentials.

2.7. Sap velocity

Sap velocity was measured in 24 trees from 2009 to 2016 using the thermal dissipation method (Granier, 1988). These trees were the same ones whose water potentials were monitored. Four *Q. ilex* and four *P. halepensis* trees were monitored in each of the three plots (Table S3). Continuous measurements of sap velocity were performed with sensors constructed at our laboratory, consisting of two probes (2 mm in diameter and 2 cm long), each containing a thermocouple to measure the stem temperature. The two probes were inserted radially into the sapwood of each tree at 1.50 m above the ground and 2 cm deep. The probes were placed 10 cm apart and covered by an aluminium reflective foil to protect them from radiation and rain.

According to sapwood length estimated with trunk ERT measurements, Granier probes measured at least 50 % of the active sapwood water flow for both species. Based on Cohen et al. (2008), sap velocities decreases with sapwood depth and is highest inner the first 2 cm of sapwood for both species, where probes are located. This gives confidence that granier sensors can detect shifts in sap velocity due to environmental factors.

The upper probe was heated constantly using a 0.12 A current. Reference measurements of the sapwood temperature were taken from the lower probe. The difference in temperature between the probes (ΔT) was recorded at 30 min intervals. Disfunctionning sensors were replaced and the affected data were excluded. Data were also lost because of power failure (animal predation, battery failure). Anomalies in ΔT fluctuations were visually identified by

overlaying the measurements with potential evapotranspiration (PET) data (calculated using the Penman-Monteith equation). When the PET increases (during daytime), ΔT decreases because of the cooling effect of sap flow on the probes.

The sap velocity (u, in $m.s^{-1}$) was then calculated using Granier's (1988) empirical equation:

$$u = 119 \times K^{1.231}, \text{ with } K = (\Delta T_{max} - \Delta T)/\Delta T \quad (1)$$

where ΔTmax is the daily maximum temperature difference between the probes, that represents the zero-sap velocity. It is supposed to occur night-time. Days with daytime occurrence of Δ Tmax were suppress from the analysis so that only night-time values were used. In addition, to limit errors in the sap velocities due to the thermal resistivity of the wood and healing effects around the probes, two linear correction factors were applied. The first (F1) was obtained by calibrating the Granier equation (1988) to data from *P. halepensis* trees from the Font-blanche site. The correction factor for the healing effect (F2) was taken from (Wiedemann et al., 2016):

$$u_{corrected} = u \times F1 \times F2 \quad (2)$$

with F1 = 1.35 and F2 = 1.53.

In the end, there was 47.7 % of missing data for the control treatment and 45.4 % for the rainfall exclusion one's. The proportion of data when sensors were working on less than three trees amounted to 24/27 % for *P. halepensis* and *Q. ilex* respectively in the control treatment, against 71/34 % in the exclusion one's. The higher proportion of missing data in the exclusion treatment was due to the lower number of monitored trees (4 against 8 in the control treatment) and to the use of CR10X Campbell to acquire the data, which are older and more subjected to power outage. It was higher for *P. halepensis* because one tree had a malfunctioning sensor for two years.

To smooth out the impact of gaps in sap velocities, we applied a moving average on sap velocity data using a 2 weeks window for each tree monitored. The PAR quantile 0.9 was calculated for each two-week period and sap velocity data was kept if they corresponded to a

PAR > q0.9 PAR. This allowed to increase the time period for which a maximum number of trees data were available.

2.8. Measurement of native embolism by direct X-ray microtomography observation

Branch segments were collected in October 2015 for *P. halepensis* and in March 2018 for both species. To avoid cutting artefacts, branches larger than 40 cm for *P. halepensis* and 90 cm for *Q. ilex* were cut just before dawn, immediately recut under water, and the cut surface was kept under water. Short (length < 4 cm length and diameter < 0.7 cm), 2-year-old sub-samples were then recut under water, immersed in liquid paraffin and stored at 4°C until analysis. The measurements were performed using the standard protocol described by Cochard et al. (2015). Each sample was positioned in the X-ray microtomograph (Nanotom 180 XS; GE, Wunstorf, Germany) and was analysed using the following settings: field of view, 5 × 5 × 5 mm^3; X-ray voltage and current, 60 kV and 240 µA; scan time, 21 min. After 3D-reconstruction, the final spatial resolution of the 3D images was 2.5 µm. One transversal 2D slice was extracted from the middle of the volume using VGStudio Max© software (Volume Graphics, HeiΔberg, Germany). The slice was then analysed using the software ImageJ (Schneider et al., 2012), to estimate the surface area of embolized conduits.

To estimate the embolism ratio for *P. halepensis*, we developed a process consisting in separating areas with embolized tracheids from areas with water-filled tracheids, which are easy to identify based on colour thresholds. The embolism ratio was then calculated as the proportion of the total cross-sectional area containing embolized tracheids (Choat et al., 2015; Torres-Ruiz et al., 2016). This procedure assumes that all tracheids have similar diameters and thus similar hydraulic conductivities. For *Q. ilex*, which is semi ring-porous, and has a lognormal distribution of conduit sizes, we first isolated large embolized vessels (which contribute the most to hydraulic conductivity) and measured their surface area to estimate the

corresponding mean diameter and hydraulic conductivity. We then used a second scan, performed on cut samples, after the free water was removed from the lumens, to estimate the diameter of all large vessels and thus the maximal hydraulic conductivity. Finally, the level of embolism was calculated as the ratio of the embolized and maximum hydraulic conductivity.

2.9. Statistics

All statistical tests were performed using the tree as the independent statistical unit, except for PAI for which it was the treatment (2 merged plots for the control treatment and one for the rainfall exclusion). Tests were only conducted if a minimum of three trees per species and treatment were available.

We used a linear mixed effect model to test the rainfall exclusion effect on sap velocity, in order to account for a potential bias causing by the low number of trees monitored, especially in the exclusion plot. Treatments, years and the interactions between treatment and years were chosen as fixed factors and trees as random factor. For the sap velocities, we also investigated whether the difference between treatments changed over time by computing the standardized difference between the maximal (spring/autumn times) values. To assess the period of the year when differences between treatments were significant, we also performed Wilcoxon rank sum tests for sap velocity considering daily moving average values of at least 3 trees per treatment under a period of 15 days.

In addition, we used a linear mixed effect model to test for a rainfall exclusion and species effect on $\Delta\Psi$. We used treatment, species, predawn water potential and included the interaction between these variables as explanatory variables, and trees as random factor. We additionally tested the rainfall exclusion effect at each measurement date for shoot water potentials, sap flow driving force ($\Delta\Psi$), native embolism and primary growth using non-parametric Wilcoxon rank sum test to overcome small sample size limitations.

Secondary growth was modelled for the two species by multiple linear regression, using the BAI calculated from the annual forest inventories as the dependent variable. The explanatory variables were the treatment, the diameter at breast height (DBH) at the beginning of the rainfall exclusion period (i.e. 2009), and the interaction between these variables. The primary growth data were analysed by comparing annual values for each branch type. The first two years of data were excluded as they contain most of the age-related signal (Fig. A2). Finally, we tested for a time effect on the evolution of PAI under both treatments, and on the difference in PAI between treatments, using a simple linear model with time as the explanatory factor. All statistical analyses were performed with the software R (3.5.2, R Development Core Team 2018).

3. Results

3.1. Effect of rainfall exclusion on tree water status

In 2008, before rainfall exclusion began, predawn water potentials (Ψ_{pd}) were similar between treatments either for *P. halepensis* or *Q. ilex.* Among the 5 sampling dates of 2008 (Fig. S5), only one was significant ($p < 0.05$), at the beginning of the dry season, when Ψ_{pd} was higher in the exclusion plot. In subsequent years, rainfall exclusion was associated with a general, although not permanent, decrease in water potentials for both species. For *Q. ilex*, Ψ_{pd} differed significantly between treatments all along the gradient of Ψ_{pd} values (Fig. 2), although the differences in Ψ_{pd} between treatments were largest (0.6 MPa) at intermediary

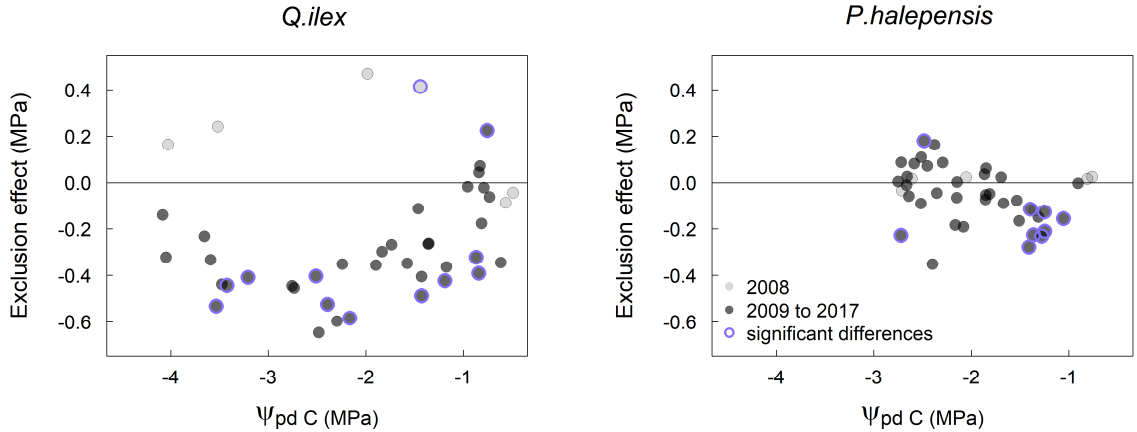

stress levels (Ψ_{pd} between –2 and –3 MPa). At more pronounced stress levels, the difference between treatments decreased to 0.2 MPa. For *P. halepensis*, Ψ_{pd} differed significantly between treatments mainly at low stress levels (Ψpd > –2 Mpa) and only occasionally at lower values (Fig. 2). The maximum difference between treatments was 0.3 MPa and occurred at higher Ψ_{pd} values than for *Q. ilex* (Ψ_{pd} of around –1.5 MPa).

Fig. 2. Effect of rainfall exclusion on the predawn leaf water potentials of *Q. ilex* and *P. halepensis*. The exclusion effect is computed as the difference between the predawn water potentials ($\Psi_{pd}^{e} - \Psi_{pd}^{c}$) in exclusion ($\Psi_{pd}^{e}$) and control trees ($\Psi_{pd}^{c}$). Each point represents the average value in a given plot on a given date. The light grey circles represent data from 2008, before rainfall exclusion was initiated, and the dark grey circles represent the values measured between 2009 and 2017. Significant differences between treatments ($p < 0.05$) are shown as purple circles.

3.2*. Effect of rainfall exclusion on sap velocities*

Bimodal seasonal variations in sap velocity were observed every year for both species and treatments, the highest values occurring during spring (from April to June), followed by a sharp decrease in summer in parallel to the corresponding decrease in soil water levels (Fig. S6-S7). A second peak occurred in autumn, concurrently with increased rainfall, and was followed by another decrease in winter (Fig. 3 and Fig. S8). Sap velocities were significantly lower in the rainfall exclusion plot for both species ($p < 0.001$ for both species considering linear mixed effect model, Table 1). Sap velocity was lower in the rainfall exclusion plot from the very first year of treatment (2009, Fig. 3-S8 reporting Wilcoxon rank sum test results), although differences between treatments were not significant from January to March for *P.halepensis* and from January to May for *Q.ilex* (3 to 5 months after the onset of rainfall exclusion). The magnitude of the average reduction in sap velocity caused by rainfall exclusion differed between years and species. The mean standardized difference in maximal (spring and autumn times) sap velocities between the control and the dry treatments shows

that *P. halepensis* sap velocities were more affected by the rainfall exclusion, for which values are between -0.3 and -0.6 while for *Q. ilex* they are comprise between -0.2 and -0.4 (Fig. S9). In addition, the mean standardized difference in maximal sap velocities remains in the same range for both species without showing any trends across years. (Fig. S9).

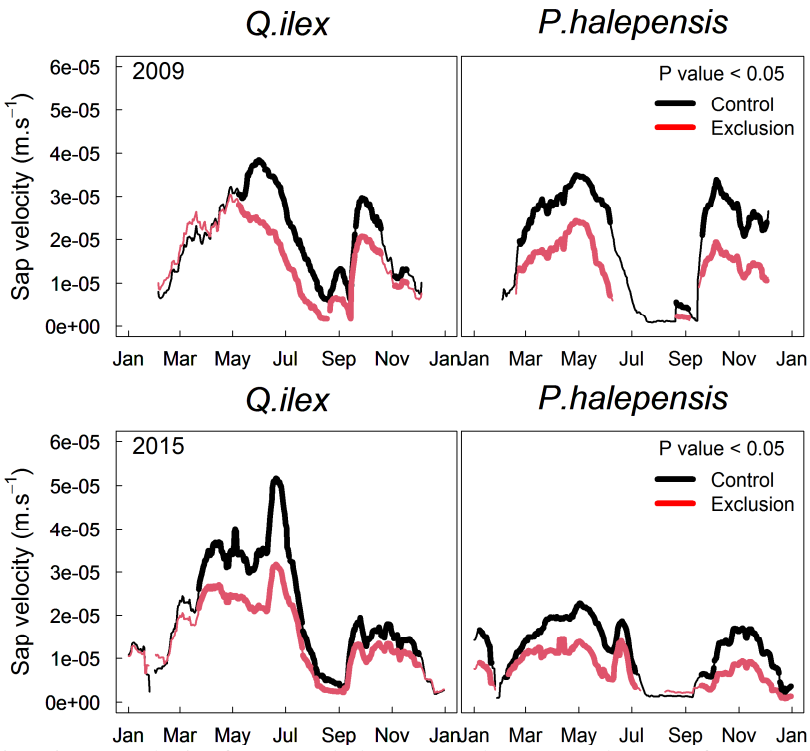

Fig. 3. Variations in sap velocity for *Pinus halepensis* and *Quercus ilex* trees from the control (black lines) and rainfall exclusion (red lines) plots, during a moderately dry year (2009) and a severely dry year (2015). For each treatment and species, the moving mean sap velocity was calculated based on data from at least three trees, over with a 2-week window. The bold lines represent periods where significant ($p < 0.05$) differences were found between treatments using Wilcoxon rank sum test. Data for all other years are shown in Fig. S8.

Table 1

Analyse of deviance table using Type III Wald chisquare tests for linear mixed effect model of sap velocity with a tree random factor.

Species	Fixed factors	Chisq	df	Pr (>Chisq)
Quercus ilex	Intercept	0.5114	1	<0.001
	Treatment	10.2381	1	<0.001
	Years	0.5736	1	<0.001
	Treatment:years	10.1591	1	<0.001

Pinus halepensis	Intercept	54.0281	1	< 0.001
	Treatment	4.8824	1	< 0.001
	Years	53.5799	1	<0.001
	Treatment:years	4.7796	1	< 0.001

3.3. *Effect of rainfall exclusion on sap flow driving force and xylem native embolism*

To further investigate the decrease in sap velocities associated with rainfall exclusion, we assessed the effect of Ψ_{pd} on the driving force for transpiration ($\Delta\Psi$). Summer $\Delta\Psi$ levels tended to be lower in the exclusion plot for both species, with more significant differences for *Q. ilex* than for *P. halepensis* (Fig. 4). $\Delta\Psi$ decreased strongly with decreasing values of Ψ_{pd} (p < 0.001, Table S4), with a significant difference in this relationship between species (p < 0.001, Table S4). For *P. halepensis*, $\Delta\Psi$ decreased linearly down to zero at –3 MPa, whereas for *Q. ilex* it decreased exponentially and then remained constant, at approximately 0.5 MPa, for Ψ_{pd} lower than –3 MPa (Fig 5a, b). There was no significant association between rainfall exclusion

and the decline in $\Delta\Psi$ with decreasing Ψ_{pd} (Fig. 5a, b and Table S4).

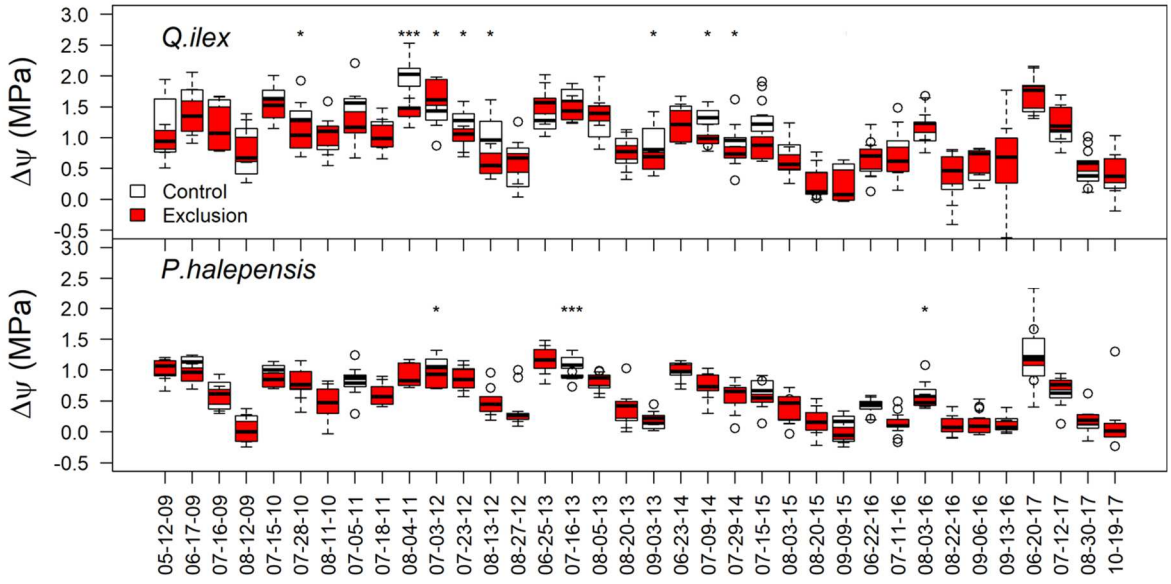

Fig. 4. Sap flow driving force (i.e. the difference between predawn and midday water potentials; $\Delta\Psi$) in *Quercus ilex* and *Pinus halepensis* trees. Sap velocity was also monitored in these trees. Each point represents

one tree at one date. Significant differences (Wilcoxon rank sum tests) are indicated by asterisks (*, $0.01 \leq p < 0.05$; ***, $p < 0.001$).

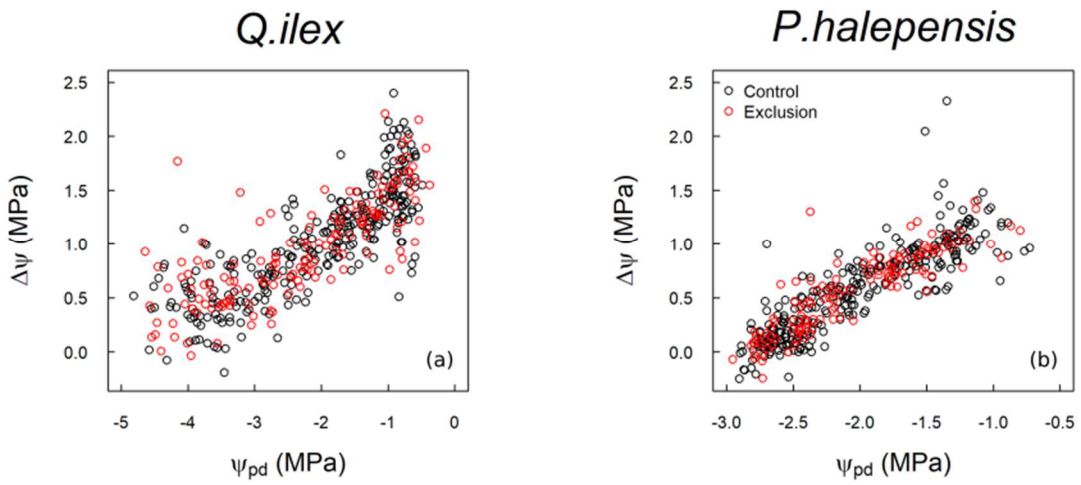

Fig 5. Variations in the sap flow driving force (difference between predawn and midday water potentials, ΔΨ) as a function of Ψ_{pd} for *Quercus ilex* (a) and *Pinus halepensis* (b).

Stem native embolism did not differ significantly between treatments for any species ($p > 0.05$, Wilcoxon rank sum test, Fig. 6). The embolism ratio, calculated from the percentage loss of theoretical conductivity, averaged 21% in March 2018 for *Q. ilex*. For *P. halepensis*, the

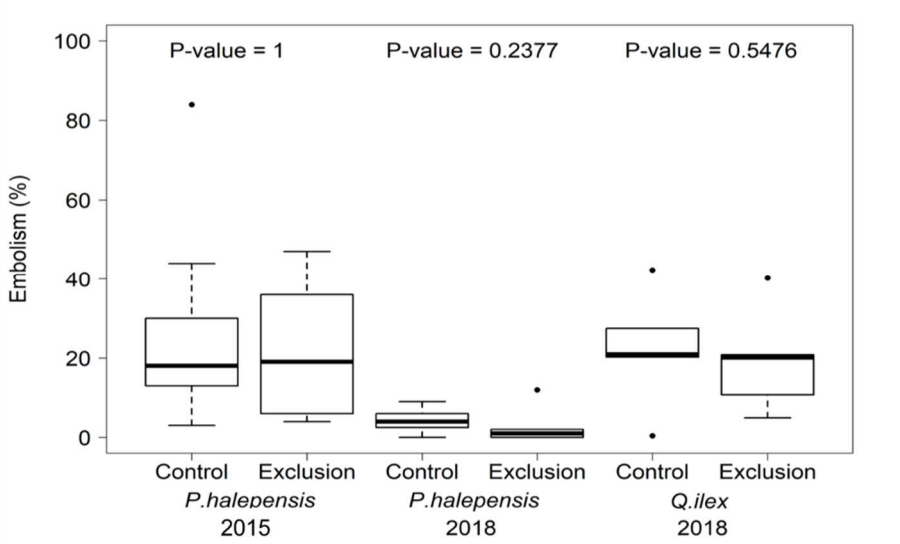

embolism ratio averaged 25% after the summer drought of 2015 but was only 4% in March 2018; this is likely due to autumn or winter growth, which is common for this species.

Fig. 6. Comparison of native stem embolism in *Pinus halepensis* and *Quercus ilex* trees in the rainfall exclusion and control plots, estimated from X-ray microtomography measurements performed in September 2015 (for both species) and in March 2018 (for *P. halepensis*).

3.4. Effect of rainfall exclusion on tree growth and plant area index

From 2009 to 2017, the annual basal area increment (BAI) of individual stems was significantly lower in the rainfall exclusion plot for *Q. ilex* trees (p = 0.04, Fig. 7 and Table S5) but not for *P. halepensis* (p = 0.68, Fig. 7 and Table S5).

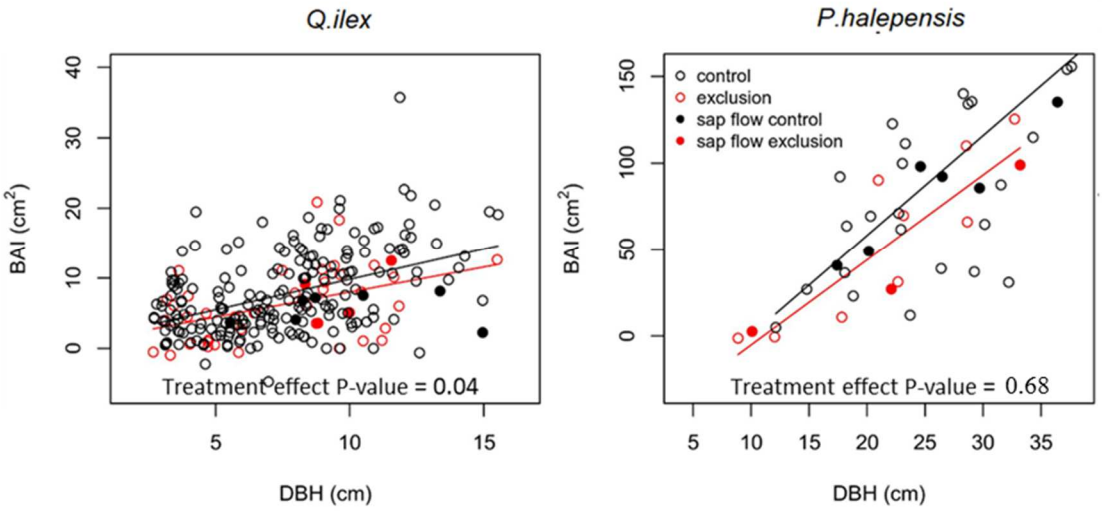

Fig. 7. Relationships between basal area increment (BAI) from 2009 to 2017 and diameter at breast height (DBH) in 2009 for *Quercus ilex* and *Pinus halepensis* trees in the control and rainfall exclusion plots. The data

from trees equipped with sap flow sensors are shown as filled circles. For *Q. ilex*, the data from coppiced stems are shown as separate points. Note that the two panels have different scales.

According to the accuracy of the sapwood delineation using ERT measurements in comparison to water profiles under cores (Fig. S4), sapwood ERT estimations were used to see if sapwood area proportion under the stem was affected by the rainfall exclusion. For both species, no significant difference between treatment was found for sapwood area/basal area ratio (p = 0.94 for *Q. ilex*, p = 0.6 for *P. halepensis*, Fig. 8 and Table S6). The significant radial growth reduction found for *Q. ilex* of the rainfall exclusion treatment imply reduced sapwood area compared to control trees.

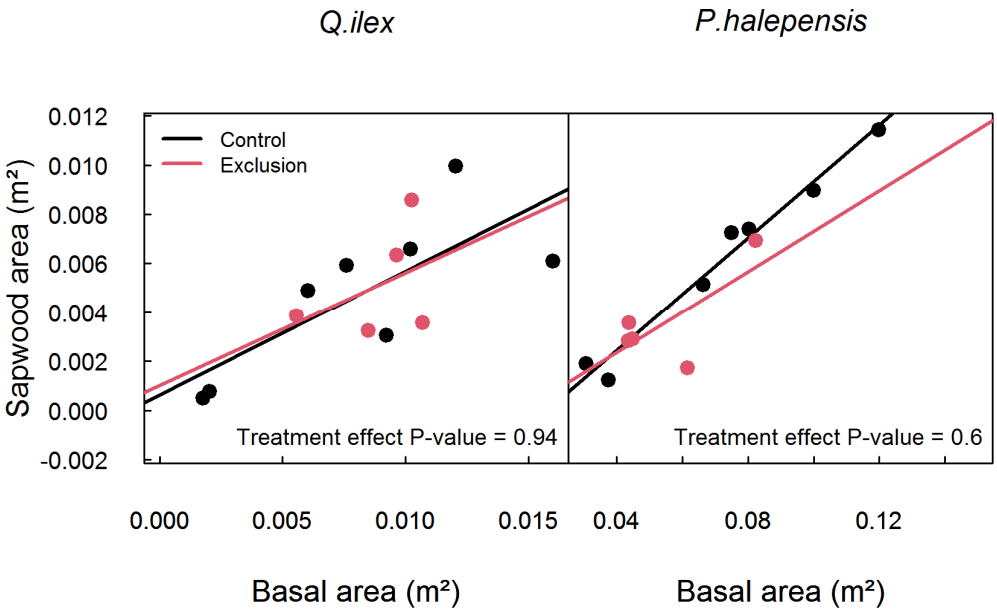

Fig. 8. Relationships between total sapwood area and basal area for *Quercus ilex* and *Pinus halepensis* trees in the control (black lines and circles) and rainfall exclusion plots (red lines and circles).

For *P. halepensis, n*eedle lengths were shorter in the rainfall exclusion plot between 2009 and 2017, especially for third-order branches for whom differences between treatment and control trees where significant for all years studied (Fig. 9a and Fig. A3 a). In the retrospectively estimated primary growth data for the 2000–2008 period (before the start of the experiment), annual shoot lengths and number of ramifications for third and second order branches were higher in the exclusion plot than in the control plots (Fig. 9c; Fig A3 b, c, d).

Shoot lengths became similar in the two groups after the start of the experiment (Fig 9c and Fig A3 b). The number of ramifications on second-order branches remained higher in the exclusion plot, as was the case well before the start of the experiment, with no clear temporal trend (Fig A3 c). The number of ramifications on third-order branches decreased over time in the rainfall exclusion plot, and reached values similar to those in the control plots from 2010 (Fig. A3 d, $p < 0.05$ before 2010, $p > 0.05$ after 2010 for all but one year; Wilcoxon rank sum tests). The decrease in the shoot length of third order branches followed a similar trend as observed for the number of ramifications (Fig. 9c). For *Q. ilex*, when the data for all branches were analysed together, there were no significant differences between treatments for either of the primary growth metrics (number of ramifications and shoot length, not shown). However, considering upper and lower canopy branches separately some differences appeared (Fig. 9 and Fig. A4). The number of ramifications on top canopy branches was significantly lower in the exclusion plot after (but not before) the start of the experiment (Fig. A4). Shoot of upper canopy branches were more numerous in the exclusion before the start of the experiment but the difference tended to decrease after the setup of the exclusion (Fig. 9d).

At the stand level, the plant area index (PAI), a surrogate of canopy cover, was higher in the rainfall exclusion plot before the start of the experiment and remained higher during the first 3 years of rainfall exclusion, after which it tended to converge with the value in the control plot (Fig. 9e). None of the year-by-year differences in PAI between treatment groups are statistically significant; however, the decrease in the PAI difference between groups during the exclusion experiment, down to zero in 2017, was significant ($p < 0.05$; Fig. 9f).

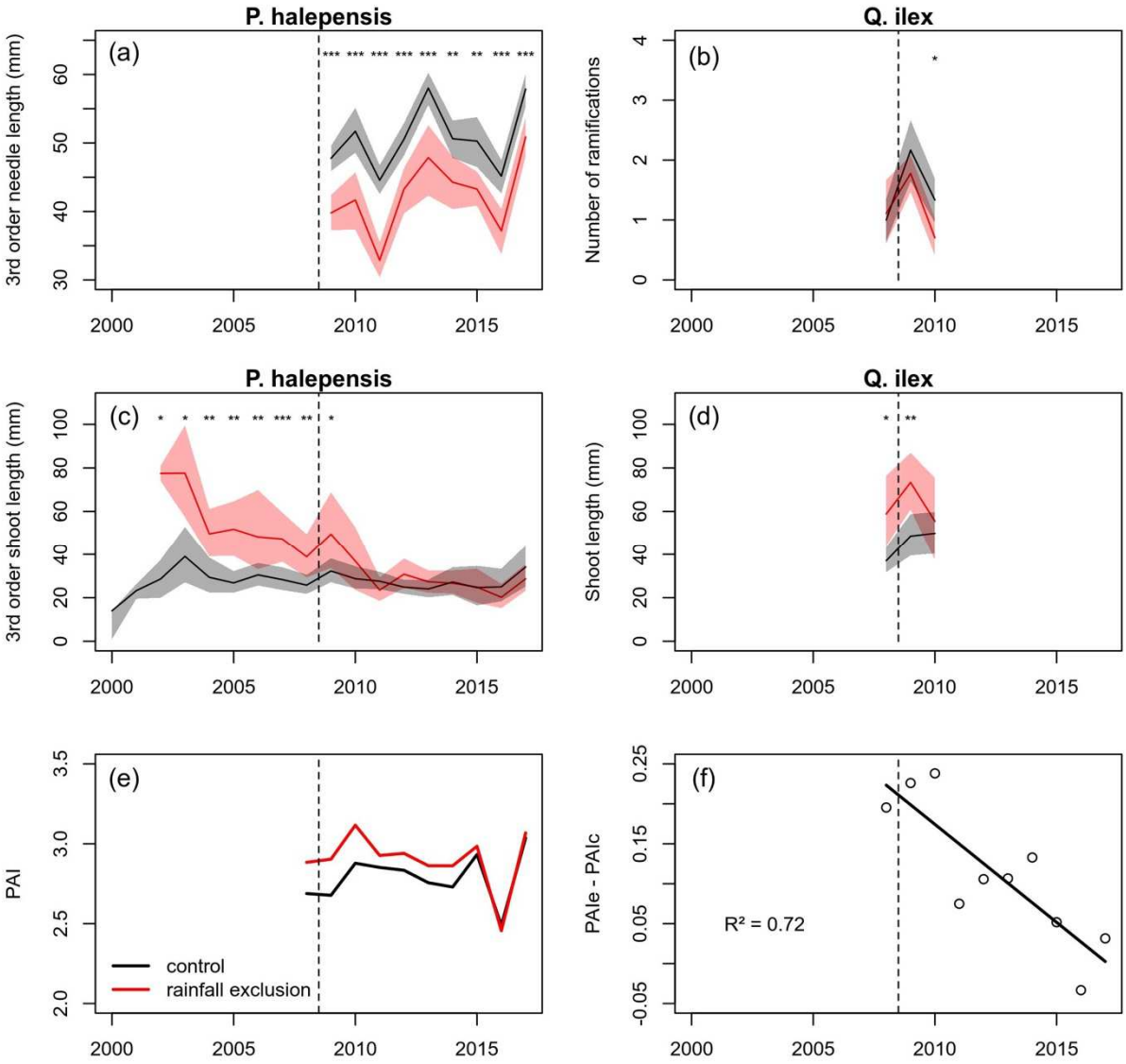

Fig. 9. Time evolution of (a) needle length, (b) number of ramifications and (c, d) shoot length for (a, c) *Pinus halepensis* and (b, d) *Quercus ilex* trees in the control (black) and rainfall exclusion (red) plots; (e) plant area index (PAI, stand-level canopy coverage) in the two plots, and (f) the difference between the PAI in the exclusion (PAIe) and control (PAIc) plots. The dashed lines indicate the start of rainfall exclusion (2009). For *Quercus ilex* only data for upper canopy branches are shown; data are presented for lower canopy branches in Fig. A4. In graphs (a) to (d), significant differences between treatments are displayed for P<0.001 (***), P<0.01 (**) and P<0.05 (*). The slope of the difference in PAI between treatments in (f) is significant (P<0.05).

4. Discussion

Assessing how trees in mixed Mediterranean forests respond to an experimental increase in drought over long timescales can provide a better understanding of how increasingly dry conditions associated to climate change in some areas is affecting forest function and succession. This 9-year rainfall exclusion experiment in a mixed pine–oak Mediterranean forest explored long-term changes in water potential, sap velocity, sap flow driving force and growth at the tree and forest level. In line with previous long-term rainfall exclusion studies (Hudson et al., 2017; Limousin et al., 2009; Maggard et al., 2016; Saunier et al., 2018) our exclusion design lead to a decrease in summer tree water potential from the very first year of the experiment in both species. We first discuss the direct effects of the rainfall exclusion treatment on summer water potentials and their consequences for tree growth and sap velocities. We then discuss the indirect effects of rainfall exclusion on the long-term decrease in sap velocities in relation to hydraulic adjustments that potentially reflect acclimation to higher drought stress.

4.1. Exclusion effects on growth

Our data support that the rainfall exclusion negatively affected the different estimates of growth we considered, in accordance with the high sensitivity of cell growth to drought (Guillemot et al., 2015; Lempereur et al., 2015). For *P. halepensis*, lower needle lengths were recorded from the very first year of the experiment onwards. On average, needles were shorter in the exclusion plot by 15.0% in 2009, and by 15.7% over the entire period. This direct effect on needle length is consistent with the results of several studies (e.g. Adams et al., 2015; Myers, 1988) that have shown that needle growth depends strongly on the water potential, notably for *P. halepensis* (Borghetti et al., 1998). The impact of rainfall exclusion on shoot length, and to a lesser extent, on the number of lateral ramifications, was delayed by at least

584 one year (Fig. 9, Fig. A3, Fig. A4). This delayed effect fits with the fact that shoot length and
585 ramification are partly predetermined in buds (Girard et al., 2012). From 2009 to 2017, trees
586 in the exclusion plot did not have shorter shoots or fewer ramifications than those in the
587 control plot, but this is mainly because they were more vigorous before the treatment started.
588 Nevertheless, there was a strong reduction in both variables once rainfall exclusion was
589 initiated for third order branches. These reductions in shoot length and needle length clearly
590 support a reduction in the leaf area for this category of branches, which are the most abundant
591 at the crown level, and account for most of the transpiration and the photosynthesis, while
592 second order branches are more involved in space exploration (Barthélémy & Caraglio,
593 2007). For *Q. ilex*, the dataset was more limited and a drought effect was only observed in the
594 number of ramifications of top branches, which slightly decreased in trees subjected to the dry
595 treatment. This decrease is in agreement with previous studies on this species (Limousin et al.,
596 2012; Martin-StPaul et al., 2013; Ogaya et al., 2006). Measurements of the PAI were in line
597 with the primary growth data, indicating a progressive reduction in the overall stand foliage
598 cover in the exclusion plot. Indeed, while the PAI in the exclusion plot was higher before the
599 start of the experiment, this difference decreased as the experiment went on, indicating a
600 progressive reduction in leaf area under rainfall exclusion.

601 The results obtained for basal area increment were not fully consistent with those on
602 primary growth, as basal area growth was only significantly reduced under rainfall exclusion
603 in *Q. ilex* and not in *P. halepensis*. *P. halepensis* and *Q. ilex* probably allocate their biomass
604 differently in response to increased drought. It is difficult to be more specific in the absence of
605 more adequate data. However, both species are known to display some plasticity in their
606 growth patterns in relation to drought. For instance, Gavinet et al. (2019) found that for *Q.*
607 *ilex*, a long-term rainfall exclusion impacted net primary productivity through a reduction in
608 leaf growth and acorn production, but not wood production. Alfaro-Sánchez et al. (2015)

609 studied differences in allometric relationships for Aleppo pines at three sites of varying levels
610 of aridity. They found that some variables were more affected by long term site conditions,
611 such as biomass and the height-stem diameter relationship, while others were more influenced
612 by recent weather conditions, such as leaf and branch biomass, and the leaf area-stem
613 diameter relationship. As expected, root growth remains a major unknown.

614 ***4.2****. Effects of rainfall exclusion on sap velocity*

615 Regarding water transport, we found that sap velocities were lower in trees subjected to
616 rainfall exclusion. This is also a widely reported response (Besson et al., 2014; Grossiord,
617 Sevanto, Borrego, et al., 2017; Limousin et al., 2009; Pangle et al., 2015; Zhang et al., 2018).
618 Here, sap velocities were lower under exclusion treatment both during the summer dry period
619 and during well-watered periods (Fig. 3 and Fig. S8). This behaviour is probably the
620 consequence of two separate phenomena. First, short-term reduction in sap velocity can be
621 due to stomatal closure, one of the primary mechanisms of plants to limit transpiration and
622 thus water potential decreases (Bréda et al., 2006; Maseda & Fernandez, 2006). The lower
623 leaf water potentials experienced by trees in the exclusion plot during summer is thus likely
624 triggered greater stomatal closure. Second, the reduced sap velocity in the exclusion plot
625 during well-watered conditions (spring and autumn) periods may be related to changes in
626 plant hydraulic conductance, that can decrease water transport capacity even when the
627 stomata are fully open (see following section).

4.3. The effects of rainfall exclusion on the tree water relation can be explained by hydraulics and growth

To better understand the parameters involved in the adjustment of the sap velocity (u, in $m \cdot s^{-1}$) to rainfall exclusion, u can be expressed in terms of Ohm's law analogy (Tyree & Ewers, 1991):

$$u = \Delta\Psi.ks = E.LA/SA \quad (3)$$

with $\Delta\Psi$ being the sap flow driving force of a tree (in MPa), ks the sapwood based specific hydraulic conductance (in $m \cdot s^{-1} \cdot MPa^{-1}$), E the transpiration per unit leaf area (in $m^3.m^{-2}.s^{-1}$), LA the tree leaf area (in m^2) and SA the tree sapwood area (in m^2). In the following paragraphs, assuming that (i) water potentials are representative of the whole tree canopy and (ii) a steady state sap flow, we discuss how changes in $\Delta\Psi$, ks and LA/SA ratio can explain the observed differences in sap velocities between treatments, and identify mechanisms imply in these changes.

During summer drought, for both species, $\Delta\Psi$ decrease earlier in the exclusion plot, which is consistent with the reduction in sap velocity due to an earlier drought and thus an earlier stomatal closure. However, this mechanism cannot explain the reduction in sap velocities in the exclusion plot that occurs during wet periods, at high Ψ_{pd}, when $\Delta\Psi$ was similar in all treatments.

The lower sap velocities measured during wet periods for trees in the rainfall exclusion may therefore be related to a decrease in *ks*. This can occur through several mechanisms. Firstly, it is well known that xylem embolism can alter hydraulic conductance (Tyree & Sperry, 1989). However, the levels of native stem embolism were similar in the experimental and control trees. Similar levels of embolism were expected for *P. halepensis* trees, because the water stress in the two plots at the end of the summer were also similar. For *Q. ilex*, these similar embolism levels suggest either that water potential levels reached were not enough to induce

653 significant embolism differences between treatment, or that the trees in the dry plot may have
654 become more resistant to embolism. Further measurements of tree vulnerability to drought-
655 induced embolism would help to explore these questions. According to the vulnerability
656 segmentation hypothesis, leaves and roots may be more vulnerable to cavitation than branches
657 or the main stem (Johnson et al., 2016; Skelton et al., 2019; Melvin T. Tyree & Ewers, 1991;
658 Zhu et al., 2016), so cavitation events in distal parts of the plant cannot be excluded.
659 Nevertheless recent studies comparing the xylem vulnerabilities of different organs
660 (Lamarque et al., 2018; Li et al., 2020; Peters et al., 2020), report no segmentation over a
661 range of deciduous and evergreen tree species. Additionally, recent results from ongoing study
662 (Moreno et al, in prep.) show no difference between leaf and stem vulnerabilities to cavitation
663 for *Quercus ilex*. All this suggests that segmentation is unlikely to occur for both studied
664 species.
665 A second possible explanation for the decrease in *k*s is that the higher drought intensity may
666 have affected the xylem anatomy of the trees in the exclusion plot (Maseda & Fernandez,
667 2006), narrowing the xylem conduits and/or increasing cell-wall thickness and wood density
668 (Dalla-Salda et al., 2011; de Luis et al., 2011; Ladjal et al., 2005; Pasho et al., 2012). These
669 changes, which have all been observed in rainfall exclusion studies (Belien et al., 2012;
670 D'Orangeville et al., 2013), reduce the risk of cavitation, but because of the trade-off between
671 xylem efficiency and safety (Venturas et al., 2017), they may also reduce xylem-specific
672 hydraulic conductance. These modifications are not systematic however, as Limousin et al.
673 (2010a) found no such adjustments in the xylem properties of *Q. ilex* trees subjected to
674 rainfall exclusion for six years. For *P. halepensis*, Pasho et al. (2012) found that severe
675 drought reduced the production of early wood and thus the global conductivity of the xylem.
676 Further anatomical analyses will help to test these hypotheses.
677 Differences in sap velocity may also be related to changes in the leaf area to sapwood area

ratio (LA/SA). Many studies have reported a decrease in the LA/SA ratio in trees subjected to increased water stress (Carter & White, 2009; Hudson et al., 2017; Limousin et al., 2010; Mencuccini & Grace, 1995). This adjustment, which is often interpreted as a mean to improve water availability and thus the gas exchange per unit leaf area, can also reduce persistently the overall tree transpiration. While we did not directly measure the LA/SA ratio here, indirect measurements at the branch level (number and size of needles) suggest that leaf areas decreased in response to exclusion treatment. At the stand level, the initial excess in PAI in the exclusion plot disappeared progressively during the experiment, which is also indicative of a decrease in LA compared with the control plot. These trends, together with the observation that *P. halepensis* basal area growth was barely affected by the treatment, suggest that rainfall exclusion led to a decrease in the LA/SA ratio. The results for *Q. ilex* are harder to interpret because of the shorter time series of data available. Nevertheless, the conservation of the tree SA/BA ratio between treatment with decreasing primary growth under the exclusion plot attest that sapwood growth was reduced by the aggravated water stress. Hence, reduction of sap velocity could probably result of an imbalance between LA/SA, with a highest reduction of LA than SA. The greater impact of rainfall exclusion on the sap velocity of *Pinus halepensis* could also be explained by LA/SA ratio spectrum. *P. halepensis* should have lowest LA/SA ratio because of a greater decrease of LA. To prospect this hypothesis, further measurements are required. It is noteworthy to add that other factors, such as canopy microclimate, not explored under this study could also influence sap velocity of both studied species.

4.4. Conclusions and perspectives

Our study shows that a nine-year 30% reduction in rainfall in a mixed forest impacted broadly similarly adult *Q. ilex* and *P. halepensis* trees, by causing an early decrease in water potential

during the summer and reducing persistently sap velocities. These effects have been frequently reported, but here we prove that such changes are certainly not caused by cavitation but rather by changes in leaf area.

However, there are also some differences in the way species have been affected. For example, it seems that the decrease in water potential during extreme drought was much more pronounced for *Q. ilex* than for *P. halepensis* and it deserves to be explored how this translates in terms of hydraulic safety margins. This is all the more intriguing since the intensity of the reduction in sap velocity in the exclusion treatment was greater for *P. halepensis* than for *Q.ilex*, which may indicate greater resilience of the later that could be related to interactions between the two species. This should be explored in the future.

Additionally, it has to be noted that studies conducted in natural conditions are inherently affected by differences in soil (Carrière et al., 2020; Nourtier et al., 2011) and stand structure. The fine-scale spatial structure of soils can be measured by electrical tomography resistivity (Carrière et al., 2020) and canopy structures can be characterized by terrestrial LiDAR (Soma et al., 2018), and these data could be combined with 3D eco-physiological models (Simioni et al., 2016). Future studies over longer timescales with data on physiological traits involved in drought response (e.g. turgor loss points and vulnerability to cavitation) will also help to elucidate how forest function and successional trajectories are likely to be affected by climate change.

References

Adams, H. D., Collins, A. D., Briggs, S. P., Vennetier M., Dickman, L. T., Sevanto, S. A., Garcia-Forner, N., Powers, H. H., & Mcdowell, N. G. (2015). Experimental drought and heat can delay phenological development and reduce foliar and shoot growth in semiarid trees. *Global Change Biology*, *21*(11), 4210–4220. https://doi.org/10.1111/gcb.13030

Adams, H. D., Zeppel, M. J. B., Anderegg, W. R. L., Hartmann, H., Landhäusser, S. M., Tissue, D. T., Huxman, T. E., Hudson, P. J., Franz, T. E., Allen, C. D., Anderegg, L. D. L., Barron-Gafford, G. A., Beerling, D. J., Breshears, D. D., Brodribb, T. J., Bugmann, H., Cobb, R. C., Collins, A. D., Dickman, L. T., … McDowell, N. G. (2017). A multi-species synthesis of physiological mechanisms in drought-induced tree mortality. *Nature Ecology and Evolution*, *1*(9), 1285–1291. https://doi.org/10.1038/s41559-017-0248-x

Alfaro-Sánchez, R., López-Serrano, F. R., Rubio, E., Sánchez-Salguero, R., Moya, D., Hernández-Tecles, E., & De Las Heras, J. (2015). Response of biomass allocation patterns to thinning in Pinus halepensis differs under dry and semiarid Mediterranean climates. *Annals of Forest Science*, *72*(5), 595–607. https://doi.org/10.1007/s13595-015-0480-y

Baquedano, F. J., & Castillo, F. J. (2006). Comparative ecophysiological effects of drought on seedlings of the Mediterranean water-saver Pinus halepensis and water-spenders Quercus coccifera and Quercus ilex. *Trees - Structure and Function*, *20*(6). https://doi.org/10.1007/s00468-006-0084-0

Barthélémy, D., & Caraglio, Y. (2007). Plant architecture: A dynamic, multilevel and comprehensive approach to plant form, structure and ontogeny. In *Annals of Botany*. https://doi.org/10.1093/aob/mcl260

Beier, C., Beierkuhnlein, C., Wohlgemuth, T., Penuelas, J., Emmett, B., Körner, C., de Boeck, H., Christensen, J. H., Leuzinger, S., Janssens, I. a, & Hansen, K. (2012). Precipitation manipulation experiments--challenges and recommendations for the future. *Ecology Letters*, *15*(8), 899–911. https://doi.org/10.1111/j.1461-0248.2012.01793.x

Belien, E., Rossi, S., Morin, H., & Deslauriers, A. (2012). Xylogenesis in black spruce subjected to rain exclusion in the field [1] This article is one of a selection of papers from the 7th International Conference on Disturbance Dynamics in Boreal Forests. *Canadian Journal of Forest Research*, *42*(7), 1306–1315. https://doi.org/10.1139/x2012-095

760 Benson, A. R., Koeser, A. K., & Morgenroth, J. (2019). Estimating conductive sapwood area
761 in diffuse and ring porous trees with electronic resistance tomography. *Tree Physiology*,
762 *39*(3), 484–494. https://doi.org/10.1093/TREEPHYS/TPY092
763 Besson, C. K., Lobo-Do-Vale, R., Rodrigues, M. L., Almeida, P., Herd, A., Grant, O. M.,
764 Soares David, T., Schmidt, M., Otieno, D., Keenan, T. F., Gouveia, C., Mériaux, C.,
765 Chaves, M. M., & Pereira, J. S. (2014). Cork oak physiological responses to manipulated
766 water availability in a Mediterranean woodland. *Agricultural and Forest Meteorology*,
767 *184*, 230–242. https://doi.org/10.1016/j.agrformet.2013.10.004
768 Borghetti, M., Cinnirella, S., Magnani, F., & Saracino, A. (1998). Impact of long-term
769 drought on xylem embolism and growth in Pinus halepensis Mill. *Trees*, *12*(4), 187–195.
770 https://doi.org/10.1007/pl00009709
771 Bréda, N., Huc, R., Granier, A., & Dreyer, E. (2006). Temperate forest trees and stands under
772 severe drought: a review of ecophysiological responses, adaptation processes and long-
773 term consequences. *Annals of Forest Science*, *63*(6), 625–644.
774 https://doi.org/10.1051/forest:2006042
775 Carrière, S. D., Ruffault, J., Pimont, F., Doussan, C., Simioni, G., Chalikakis, K., Limousin,
776 J.-M., Scotti, I., Courdier, F., Cakpo, C.-B., Davi, H., & Martin-StPaul, N. K. (2020).
777 Impact of local soil and subsoil conditions on inter-individual variations in tree responses
778 to drought: insights from Electrical Resistivity Tomography. *Science of The Total*
779 *Environment*, *698*, 134247. https://doi.org/10.1016/J.SCITOTENV.2019.134247
780 Carter, J. L., & White, D. A. (2009). Plasticity in the Huber value contributes to homeostasis
781 in leaf water relations of a mallee Eucalypt with variation to groundwater depth. *Tree*
782 *Physiology*, *29*(11), 1407–1418.
783 Choat, B., Brodersen, C. R., & Mcelrone, A. J. (2015). Synchrotron X-ray microtomography
784 of xylem embolism in Sequoia sempervirens saplings during cycles of drought and
785 recovery. *New Phytologist*, *205*(3), 1095–1105. https://doi.org/10.1111/nph.13110
786 Choat, B., Brodribb, T. J., Brodersen, C. R., Duursma, R. A., López, R., & Medlyn, B. E.
787 (2018). Triggers of tree mortality under drought Drought and forest mortality. *Nature*,
788 *558*, 531–539. https://doi.org/10.1038/s41586-018-0240-x
789 Cochard, H., Delzon, S., & Badel, E. (2015). X-ray microtomography (micro-CT): A
790 reference technology for high-resolution quantification of xylem embolism in trees.
791 *Plant, Cell and Environment*, *38*(1), 201–206. https://doi.org/10.1111/pce.12391
792 Cohen, Y., Cohen, S., Cantuarias-Aviles, T., & Schiller, G. (2008). Variations in the radial
793 gradient of sap velocity in trunks of forest and fruit trees. *Plant and Soil*, *305*(1–2), 49–

794 59. https://doi.org/10.1007/s11104-007-9351-0
795 Cramer, W., Guiot, J., Fader, M., Garrabou, J., Gattuso, J. P., Iglesias, A., Lange, M. A.,
796 Lionello, P., Llasat, M. C., Paz, S., Peñuelas, J., Snoussi, M., Toreti, A., Tsimplis, M. N.,
797 & Xoplaki, E. (2018). Climate change and interconnected risks to sustainable
798 development in the Mediterranean. In *Nature Climate Change* (Vol. 8, Issue 11, pp. 972–
799 980). Nature Publishing Group. https://doi.org/10.1038/s41558-018-0299-2
800 D'Orangeville, L., Cote, B., Houle, D., & Morin, H. (2013). The effects of throughfall
801 exclusion on xylogenesis of balsam fir. *Tree Physiology*, *33*(5), 516–526.
802 https://doi.org/10.1093/treephys/tpt027
803 Dai, A. (2012). Increasing drought under global warming in observations and models. *Nature*
804 *Climate Change*, *3*(1), 52–58. https://doi.org/10.1038/nclimate1633
805 Dalla-Salda, G., Martinez-Meier, A., Cochard, H., & Rozenberg, P. (2011). Genetic variation
806 of xylem hydraulic properties shows that wood density is involved in adaptation to
807 drought in Douglas-fir (Pseudotsuga menziesii (Mirb.)). *Annals of Forest Science*, *68*(4),
808 747–757. https://doi.org/10.1007/s13595-011-0091-1
809 de Luis, M., Novak, K., Raventós, J., Gričar, J., Prislan, P., & Čufar, K. (2011). Cambial
810 activity, wood formation and sapling survival of Pinus halepensis exposed to different
811 irrigation regimes. *Forest Ecology and Management*, *262*(8), 1630–1638.
812 https://doi.org/10.1016/J.FORECO.2011.07.013
813 Delzon, S., Douthe, C., Sala, A., & Cochard, H. (2010). Mechanism of water-stress induced
814 cavitation in conifers: Bordered pit structure and function support the hypothesis of seal
815 capillary-seeding. *Plant, Cell and Environment*, *33*(12). https://doi.org/10.1111/j.1365-
816 3040.2010.02208.x
817 Diffenbaugh, N. S., & Giorgi, F. (2012). Climate change hotspots in the CMIP5 global
818 climate model ensemble. *Climatic Change*, *114*(3–4), 813–822.
819 https://doi.org/10.1007/s10584-012-0570-x
820 FAO and Plan Bleu. (2018). *State of Mediterranean Forests 2018* (FAO and Plan Bleu (ed.)).
821 http://www.fao.org/docrep/017/i3226e/i3226e.pdf
822 Fisher, R. A., Williams, M., da Costa, A. L., Malhi, Y., da Costa, R. F., Almeida, S., & Meir,
823 P. (2007). The response of an Eastern Amazonian rain forest to drought stress: Results
824 and modelling analyses from a throughfall exclusion experiment. *Global Change*
825 *Biology*, *13*(11), 2361–2378. https://doi.org/10.1111/j.1365-2486.2007.01417.x
826 Flexas, J., Bota, J., Loreto, F., Cornic, G., & Sharkey, T. D. (2004). Diffusive and Metabolic
827 Limitations to Photosynthesis under Drought and Salinity in C3 Plants. *Plant Biology*, *6*,

269–279.

Friedlingstein, P., Jones, M. W., O'Sullivan, M., Andrew, R. M., Hauck, J., Peters, G. P., Peters, W., Pongratz, J., Sitch, S., Le Quéré, C., DBakker, O. C. E., Canadell1, J. G., Ciais1, P., Jackson, R. B., Anthoni1, P., Barbero, L., Bastos, A., Bastrikov, V., Becker, M., … Zaehle, S. (2019). Global carbon budget 2019. *Earth System Science Data*, *11*(4), 1783–1838. https://doi.org/10.5194/essd-11-1783-2019

Gavinet, J., Ourcival, J. M., & Limousin, J. M. (2019). Rainfall exclusion and thinning can alter the relationships between forest functioning and drought. *New Phytologist*, *223*(3), 1267–1279. https://doi.org/10.1111/nph.15860

Gessler, A., Cailleret, M., Joseph, J., Schönbeck, L., Schaub, M., Lehmann, M., Treydte, K., Rigling, A., Timofeeva, G., & Saurer, M. (2018). Drought induced tree mortality - a tree-ring isotope based conceptual model to assess mechanisms and predispositions. *New Phytologist*, *219*(2), 485–490. https://doi.org/10.1111/nph.15154

Girard, F., Vennetier, M., Guibal, F., Corona, C., Ouarmim, S., & Herrero, A. (2012). Pinus halepensis Mill. crown development and fruiting declined with repeated drought in Mediterranean France. *European Journal of Forest Research*. https://doi.org/10.1007/s10342-011-0565-6

Granier, A. (1988). Evaluation of transpiration in a Douglas-fir stand by means of sap flow measurements. *Tree Physiology*, *3*(4), 309–320. https://doi.org/10.1093/treephys/3.4.309

Granier, A., Bréda, N., Biron, P., & Villette, S. (1999). A lumped water balance model to evaluate duration and intensity of drought constraints in forest stands. *Ecological Modelling*, *116*(2–3), 269–283. https://doi.org/10.1016/S0304-3800(98)00205-1

Grossiord, C., Sevanto, S., Adams, H. D., Collins, A. D., Dickman, L. T., McBranch, N., Michaletz, S. T., Stockton, E. A., Vigil, M., & McDowell, N. G. (2017). Precipitation, not air temperature, drives functional responses of trees in semi-arid ecosystems. *Journal of Ecology*, *105*(1), 163–175. https://doi.org/10.1111/1365-2745.12662

Grossiord, C., Sevanto, S., Borrego, I., Chan, A. M., Collins, A. D., Dickman, L. T., Hudson, P. J., McBranch, N., Michaletz, S. T., Pockman, W. T., Ryan, M., Vilagrosa, A., & McDowell, N. G. (2017). Tree water dynamics in a drying and warming world. *Plant, Cell & Environment*, *40*(9), 1861–1873. https://doi.org/10.1111/pce.12991

Grossiord, C., Sevanto, S., Limousin, J. M., Meir, P., Mencuccini, M., Pangle, R. E., Pockman, W. T., Salmon, Y., Zweifel, R., & McDowell, N. G. (2018). Manipulative experiments demonstrate how long-term soil moisture changes alter controls of plant water use. *Environmental and Experimental Botany*, *152*, 19–27.

https://doi.org/10.1016/j.envexpbot.2017.12.010

Guillemot, J., Martin-StPaul, N. K., Dufrêne, E., François, C., Soudani, K., Ourcival, J. M., & Delpierre, N. (2015). The dynamic of the annual carbon allocation to wood in European tree species is consistent with a combined source–sink limitation of growth: implications for modelling. *Biogeosciences*, *12*(9), 2773–2790. https://doi.org/10.5194/bg-12-2773-2015

Guyot, A., Ostergaard, K. T., Lenkopane, M., Fan, J., & Lockington, D. A. (2013). Using electrical resistivity tomography to differentiate sapwood from heartwood: Application to conifers. *Tree Physiology*, *33*(2), 187–194. https://doi.org/10.1093/treephys/tps128

Hudson, P. J., Limousin, | J M, Krofcheck, | D J, Boutz, | A L, Pangle, | R E, Gehres, | N, Mcdowell, | N G, & Pockman, | W T. (2017). *Impacts of long-term precipitation manipulation on hydraulic architecture and xylem anatomy of piñon and juniper in Southwest USA*. https://doi.org/10.1111/pce.13109

Johnson, D. M., Wortemann, R., McCulloh, K. A., Jordan-Meille, L., Ward, E., Warren, J. M., Palmroth, S., & Domec, J.-C. (2016). A test of the hydraulic vulnerability segmentation hypothesis in angiosperm and conifer tree species. *Tree Physiology*, *36*(8), 983–993. https://doi.org/10.1093/treephys/tpw031

Kawaletz, H., Mölder, I., Annighöfer, P., Terwei, A., Zerbe, S., & Ammer, C. (2014). Pot experiments with woody species - A review. In *Forestry*. https://doi.org/10.1093/forestry/cpu017

Klein, T., Di Matteo, G., Rotenberg, E., Cohen, S., & Yakir, D. (2013). Differential ecophysiological response of a major Mediterranean pine species across a climatic gradient. *Tree Physiology*, *33*(1), 26–36. https://doi.org/10.1093/treephys/tps116

Klepsch, M., Zhang, Y., Kotowska, M. M., Lamarque, L. J., Nolf, M., Schuldt, B., Torres-Ruiz, J. M., Qin, D. W., Choat, B., Delzon, S., Scoffoni, C., Cao, K. F., & Jansen, S. (2018). Is xylem of angiosperm leaves less resistant to embolism than branches? Insights from microCT, hydraulics, and anatomy. *Journal of Experimental Botany*, *69*(22). https://doi.org/10.1093/jxb/ery321

Köhler, M., Schwendenmann, L., & Hölscher, D. (2010). Throughfall reduction in a cacao agroforest: tree water use and soil water budgeting. *Agricultural and Forest Meteorology*, *150*, 1079–1089. https://doi.org/10.1016/j.agrformet.2010.04.005

Ladjal, M., Huc, R., & Ducrey, M. (2005). Drought effects on hydraulic conductivity and xylem vulnerability to embolism in diverse species and provenances of Mediterranean cedars. *Tree Physiology*, *25*(9), 1109–1117.

Lamarque, L. J., Corso, D., Torres-Ruiz, J. M., Badel, E., Brodribb, T. J., Burlett, R., Charrier, G., Choat, B., Cochard, H., Gambetta, G. A., Jansen, S., King, A., Lenoir, N., Martin-StPaul, N., Steppe, K., Van den Bulcke, J., Zhang, Y., & Delzon, S. (2018). An inconvenient truth about xylem resistance to embolism in the model species for refilling Laurus nobilis L. *Annals of Forest Science*, *75*(3). https://doi.org/10.1007/s13595-018-0768-9

Leblanc, S. G., Chen, J. M., Fernandes, R., Deering, D. W., & Conley, A. (2005). Methodology comparison for canopy structure parameters extraction from digital hemispherical photography in boreal forests. *Agricultural and Forest Meteorology*, *129*(3–4), 187–207. https://doi.org/10.1016/j.agrformet.2004.09.006

Lempereur, M., Martin-stpaul, N. K., Damesin, C., Joffre, R., Ourcival, J.-M., Rocheteau, A., & Rambal, S. (2015). Growth duration rather than carbon supply explains the stem increment of Quercus ilex : Implication for vulnerability assessment under climate change. *New Phytologist*, *33*(0), 1–42. https://doi.org/10.1111/nph.13400

Li, X., Delzon, S., Torres-Ruiz, J., Badel, E., Burlett, R., Cochard, H., Jansen, S., King, A., Lamarque, L. J., Lenoir, N., St-Paul, N. M., & Choat, B. (2020). Lack of vulnerability segmentation in four angiosperm tree species: evidence from direct X-ray microtomography observation. *Annals of Forest Science*, *77*(2). https://doi.org/10.1007/s13595-020-00944-2

Limousin, J.-M., Longepierre, D., Huc, R., & Rambal, S. (2010). Change in hydraulic traits of Mediterranean Quercus ilex subjected to long-term throughfall exclusion. *Tree Physiology*, *30*(8), 1026–1036. https://doi.org/10.1093/treephys/tpq062

Limousin, J.-M., Misson, L., Lavoir, A.-V., Martin, N. K., & Rambal, S. (2010). Do photosynthetic limitations of evergreen Quercus ilex leaves change with long-term increased drought severity? *Plant, Cell & Environment*, *33*(5), 863–875. https://doi.org/10.1111/j.1365-3040.2009.02112.x

Limousin, J.-M., Rambal, S., Ourcival, J.-M., Rodríguez-Calcerrada, J., Pérez-Ramos, I. M., Rodríguez-Cortina, R., Misson, L., & Joffre, R. (2012). Morphological and phenological shoot plasticity in a Mediterranean evergreen oak facing long-term increased drought. *Oecologia*, *169*(2), 565–577. https://doi.org/10.1007/s00442-011-2221-8

Limousin, J. M., Rambal, S., Ourcival, J. M., Rocheteau, A., Joffre, R., & Rodriguez-Cortina, R. (2009). Long-term transpiration change with rainfall decline in a Mediterranean Quercus ilex forest. *Global Change Biology*, *15*(9), 2163–2175. https://doi.org/10.1111/j.1365-2486.2009.01852.x

930 Lionello, P., & Scarascia, L. (2018). The relation between climate change in the
931 Mediterranean region and global warming. *Regional Environmental Change*, *18*(5),
932 1481–1493. https://doi.org/10.1007/s10113-018-1290-1
933 Lobo, A., Torres-Ruiz, J. M., Burlett, R., Lemaire, C., Parise, C., Francioni, C., Truffaut, L.,
934 Tomášková, I., Hansen, J. K., Kjær, E. D., Kremer, A., & Delzon, S. (2018). Assessing
935 inter- and intraspecific variability of xylem vulnerability to embolism in oaks. *Forest*
936 *Ecology and Management*, *424*. https://doi.org/10.1016/j.foreco.2018.04.031
937 Maggard, A., Will, R., Wilson, D., & Meek, C. (2016). Response of Mid-Rotation Loblolly
938 Pine (Pinus taeda L.) Physiology and Productivity to Sustained, Moderate Drought on
939 the Western Edge of the Range. *Forests*, *7*(12), 203. https://doi.org/10.3390/f7090203
940 Martín-Benito, D., Cherubini, P., Del Río, M., & Cañellas, I. (2008). Growth response to
941 climate and drought in Pinus nigra Arn. trees of different crown classes. *Trees -*
942 *Structure and Function*, *22*(3), 363–373. https://doi.org/10.1007/s00468-007-0191-6
943 Martin-StPaul, N., Delzon, S., & Cochard, H. (2017). Plant resistance to drought depends on
944 timely stomatal closure. *Ecology Letters*, *20*(11), 1437–1447.
945 https://doi.org/10.1111/ele.12851
946 Martin-StPaul, N. K., Limousin, J.-M., Vogt-Schilb, H., Rodríguez-Calcerrada, J., Rambal,
947 S., Longepierre, D., & Misson, L. (2013). The temporal response to drought in a
948 Mediterranean evergreen tree: comparing a regional precipitation gradient and a
949 throughfall exclusion experiment. *Global Change Biology*, *19*(8), 2413–2426.
950 https://doi.org/10.1111/gcb.12215
951 Martin-Stpaul, N. K., Limousin, J. M., Rodrígesuez-Calcerrada, J., Ruffault, J., Rambal, S.,
952 Letts, M. G., & Misson, L. (2012). Photosynthetic sensitivity to drought varies among
953 populations of Quercus ilex along a rainfall gradient. *Functional Plant Biology*, *39*(1),
954 25–37. https://doi.org/10.1071/FP11090
955 Maseda, P. H., & Fernandez, R. J. (2006). Stay wet or else: three ways in which plants can
956 adjust hydraulically to their environment. *Journal of Experimental Botany*, *57*(15),
957 3963–3977. https://doi.org/10.1093/jxb/erl127
958 McDowell, N., Pockman, W. T., Allen, C. D., Breshears, D. D., Cobb, N., Kolb, T., Plaut, J.,
959 Sperry, J., West, A., Williams, D. G., & Yepez, E. A. (2008). Mechanisms of plant
960 survival and mortality during drought: why do some plants survive while others succumb
961 to drought? *New Phytologist*, *178*(4), 719–739. https://doi.org/10.1111/j.1469-
962 8137.2008.02436.x
963 McDowell, Nate G., Allen, C. D., Anderson-Teixeira, K., Aukema, B. H., Bond-Lamberty,

B., Chini, L., Clark, J. S., Dietze, M., Grossiord, C., Hanbury-Brown, A., Hurtt, G. C., Jackson, R. B., Johnson, D. J., Kueppers, L., Lichstein, J. W., Ogle, K., Poulter, B., Pugh, T. A. M., Seidl, R., … Xu, C. (2020). Pervasive shifts in forest dynamics in a changing world. *Science (New York, N.Y.)*, *368*(6494). https://doi.org/10.1126/science.aaz9463

McDowell, Nathan G. (2011). Mechanisms linking drought, hydraulics, carbon metabolism, and vegetation mortality. *Plant Physiology*, *155*(3), 1051–1059. https://doi.org/10.1104/pp.110.170704

Mencuccini, M., & Grace, J. (1995). Climate influences the leaf area/sapwood area ratio in Scots pine. *Tree Physiology*, *15*(1), 1–10.

Muller, B., Pantin, F., Génard, M., Turc, O., Freixes, S., Piques, M., & Gibon, Y. (2011). Water deficits uncouple growth from photosynthesis, increase C content, and modify the relationships between C and growth in sink organs. *Journal of Experimental Botany*, *62*(6), 1715–1729. https://doi.org/10.1093/jxb/erq438

Myers, B. J. (1988). Water-stress Integral - A Link Between Short-term Stress and Long-term Growth. *Tree Physiology*, *4*(4), 315–323.

Nourtier, M., Chanzy, A., Granier, A., & Huc, R. (2011). Sap flow measurements by thermal dissipation method using cyclic heating: a processing method accounting for the non-stationary regime. *Annals of Forest Science*, *68*(7), 1255–1264. https://doi.org/10.1007/s13595-011-0065-3

Ogaya, R., & Penuelas, J. (2007). Tree growth, mortality, and above-ground biomass accumulation in a holm oak forest under a five-year experimental field drought. *Plant Ecology*, *189*(2), 291–299. https://doi.org/10.1007/s11258-006-9184-6

Ogaya, R., Penuelas, J., Peñuelas, J., Csic-ceab-creaf, U. E., & Barcelona, U. A. De. (2006). Contrasting foliar responses to drought in Quercus ilex and Phillyrea latifolia. *Biologia Plantarum*, *50*(3), 373–382.

Pangle, R. E., Limousin, J.-M., Plaut, J. A., Yepez, E. A., Hudson, P. J., Boutz, A. L., Gehres, N., Pockman, W. T., & McDowell, N. G. (2015). Prolonged experimental drought reduces plant hydraulic conductance and transpiration and increases mortality in a piñon-juniper woodland. *Ecology and Evolution*, *5*(8), 1618–1638. https://doi.org/10.1002/ece3.1422

Pardos, M., Climent, J., Gil, L., & Pardos, J. A. (2003). Shoot growth components and flowering phenology in grafted Pinus halepensis Mill. *Trees - Structure and Function*. https://doi.org/10.1007/s00468-003-0259-x

998 Pasho, E., Julio Camarero, J., & Vicente-Serrano, S. M. (2012). Climatic impacts and drought
999 control of radial growth and seasonal wood formation in Pinus halepensis. *Trees*, *26*(6),
1000 1875–1886. https://doi.org/10.1007/s00468-012-0756-x
1001 Pellizzari, E., Camarero, J. J., Gazol, A., Sangüesa-Barreda, G., & Carrer, M. (2016). Wood
1002 anatomy and carbon-isotope discrimination support long-term hydraulic deterioration as
1003 a major cause of drought-induced dieback. *Global Change Biology*, *22*(6), 2125–2137.
1004 https://doi.org/10.1111/gcb.13227
1005 Peters, J. M. R., Gauthey, A., Lopez, R., Carins-Murphy, M. R., Brodribb, T. J., & Choat, B.
1006 (2020). Non-invasive imaging reveals convergence in root and stem vulnerability to
1007 cavitation across five tree species. *Journal of Experimental Botany*, *71*(20), 6623–6637.
1008 https://doi.org/10.1093/jxb/eraa381
1009 Rodríguez-Calcerrada, J., Pérez-Ramos, I. M., Ourcival, J.-M., Limousin, J.-M., Joffre, R., &
1010 Rambal, S. (2011). Is selective thinning an adequate practice for adapting Quercus ilex
1011 coppices to climate change? *Annals of Forest Science*, *68*(3), 575–585.
1012 https://doi.org/10.1007/s13595-011-0050-x
1013 Saunier, A., Ormeño, E., Havaux, M., Wortham, H., Ksas, B., Temime-Roussel, B., Blande, J.
1014 D., Lecareux, C., Mévy, J. P., Bousquet-Mélou, A., Gauquelin, T., & Fernandez, C.
1015 (2018). Resistance of native oak to recurrent drought conditions simulating predicted
1016 climatic changes in the Mediterranean region. *Plant Cell and Environment*.
1017 https://doi.org/10.1111/pce.13331
1018 Schneider, C. A., Rasband, W. S., & Eliceiri, K. W. (2012). NIH Image to ImageJ: 25 years of
1019 image analysis. In *Nature Methods* (Vol. 9, Issue 7, pp. 671–675). Nature Publishing
1020 Group. https://doi.org/10.1038/nmeth.2089
1021 Simioni, G., Marie, G., & Huc, R. (2016). Influence of vegetation spatial structure on growth
1022 and water fluxes of a mixed forest: Results from the NOTG 3D model. *Ecological*
1023 *Modelling*, *328*, 119–135. https://doi.org/10.1016/j.ecolmodel.2016.02.004
1024 Skelton, R. P., Anderegg, L. D. L., Papper, P., Reich, E., Dawson, T. E., Kling, M.,
1025 Thompson, S. E., Diaz, J., & Ackerly, D. D. (2019). No local adaptation in leaf or stem
1026 xylem vulnerability to embolism, but consistent vulnerability segmentation in a North
1027 American oak. *New Phytologist*, *223*(3), 1296–1306. https://doi.org/10.1111/nph.15886
1028 Soma, M., Pimont, F., Durrieu, S., & Dupuy, J.-L. (2018). Enhanced Measurements of Leaf
1029 Area Density with T-LiDAR: Evaluating and Calibrating the Effects of Vegetation
1030 Heterogeneity and Scanner Properties. *Remote Sensing*, *10*(10), 1580.
1031 https://doi.org/10.3390/rs10101580

Song, J., Wan, S., Piao, S., Knapp, A. K., Classen, A. T., Vicca, S., Ciais, P., Hovenden, M. J., Leuzinger, S., Beier, C., Kardol, P., Xia, J., Liu, Q., Ru, J., Zhou, Z., Luo, Y., Guo, D., Adam Langley, J., Zscheischler, J., … Zheng, M. (2019). A meta-analysis of 1,119 manipulative experiments on terrestrial carbon-cycling responses to global change. *Nature Ecology and Evolution*, *3*(9), 1309–1320. https://doi.org/10.1038/s41559-019-0958-3

Timofeeva, G., Treydte, K., Bugmann, H., Rigling, A., Schaub, M., Siegwolf, R., & Saurer, M. (2017). Long-term effects of drought on tree-ring growth and carbon isotope variability in Scots pine in a dry environment. *Tree Physiology*, *37*(8), 1028–1041. https://doi.org/10.1093/TREEPHYS/TPX041

Torres-Ruiz, J. M., Cochard, H., Mencuccini, M., Delzon, S., & Badel, E. (2016). Direct observation and modelling of embolism spread between xylem conduits: a case study in Scots pine. *Plant Cell and Environment*, *39*(12), 2774–2785. https://doi.org/10.1111/pce.12840

Tyree, M T, & Sperry, J. S. (1989). Vulnerability of Xylem to Cavitation and Embolism. *Annual Review of Plant Physiology and Plant Molecular Biology*, *40*(1), 19–36. https://doi.org/10.1146/annurev.pp.40.060189.000315

Tyree, Melvin T., & Ewers, F. W. (1991). The hydraulic architecture of trees and other woody plants. *New Phytologist*, *119*(3), 345–360. https://doi.org/10.1111/j.1469-8137.1991.tb00035.x

Ward, E. J., Domec, J. C., Laviner, M. A., Fox, T. R., Sun, G., McNulty, S., King, J., & Noormets, A. (2015). Fertilization intensifies drought stress: Water use and stomatal conductance of Pinus taeda in a midrotation fertilization and throughfall reduction experiment. *Forest Ecology and Management*, *355*, 72–82. https://doi.org/10.1016/j.foreco.2015.04.009

Welles, J. M., & Norman, J. M. (1991). *(1991) Instrument for Indirect Measurement of Canopy Architecture (AJ).*

Wiedemann, A., Marañón-Jiménez, S., Rebmann, C., Herbst, M., & Cuntz, M. (2016). An empirical study of the wound effect on sap flux density measured with thermal dissipation probes. *Tree Physiology*, *36*(12), 1471–1484. https://doi.org/10.1093/treephys/tpw071

Wu, Z., Dijkstra, P., Koch, G. W., Peñuelas, J., & Hungate, B. A. (2011). Responses of terrestrial ecosystems to temperature and precipitation change: A meta-analysis of experimental manipulation. In *Global Change Biology* (Vol. 17, Issue 2, pp. 927–942).

https://doi.org/10.1111/j.1365-2486.2010.02302.x

Wullschleger, S. D., & Hanson, P. J. (2006). Sensitivity of canopy transpiration to altered precipitation in an upland oak forest: evidence from a long-term field manipulation study. *Global Change Biology*, *12*(1), 97–109. https://doi.org/10.1111/j.1365-2486.2005.001082.x

Zhang, Q., Jia, X., Shao, M., Zhang, C., Li, X., & Ma, C. (2018). Sap flow of black locust in response to short-Term drought in southern Loess Plateau of China. *Scientific Reports*, *8*(1), 1–10. https://doi.org/10.1038/s41598-018-24669-5

Zhu, S.-D., Liu, H., Xu, Q.-Y., Cao, K.-F., & Ye, Q. (2016). Are leaves more vulnerable to cavitation than branches? *Functional Ecology*, *30*(11), 1740–1744. https://doi.org/10.1111/1365-2435.12656

Acknowledgements:

The data analysis and writing for this study were supported by the French Environment and Energy Management Agency (ADEME) in the form of a PhD scholarship. During the long study period, experiments were funded by the French National Research Institute for Agriculture, Food and Environment (INRAE), the Agence Nationale pour la Recherche (ANR project Drought+), the long term French observatory networks SOERE F-ORE-T and Analysis and Experimentation on Ecosystems (AnaEE). The authors thank Damien Gounelle, Arnaud Jouineau, Jean-Michel Lopez, Mathieu Audouard, and Roland Esteve, from INRAE, for their contributions to the field work. The authors also thank the INRAE PHENOBOIS centre (Clermont-Ferrand, France) and Pierre Conchon for help with the X-ray microtomography analysis.

Appendices

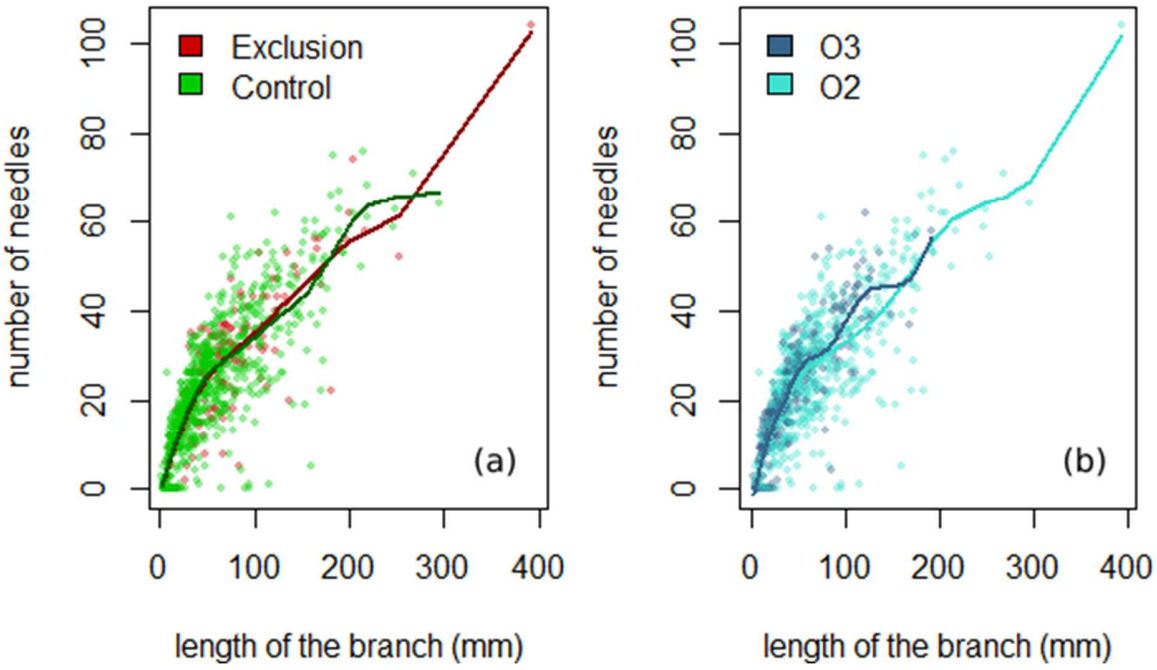

Fig. A1. Number of needles vs branch length compared between (A) rainfall exclusion and control trees and (B) branch architectural order (O2 vs O3). The lines are general additive models fitted to the data and show that the relationship between needle number and branch length does not depend on rainfall or architectural order. The data were collected in autumn 2009 on a sample of 953 branches that grew in 2008 and 2009.

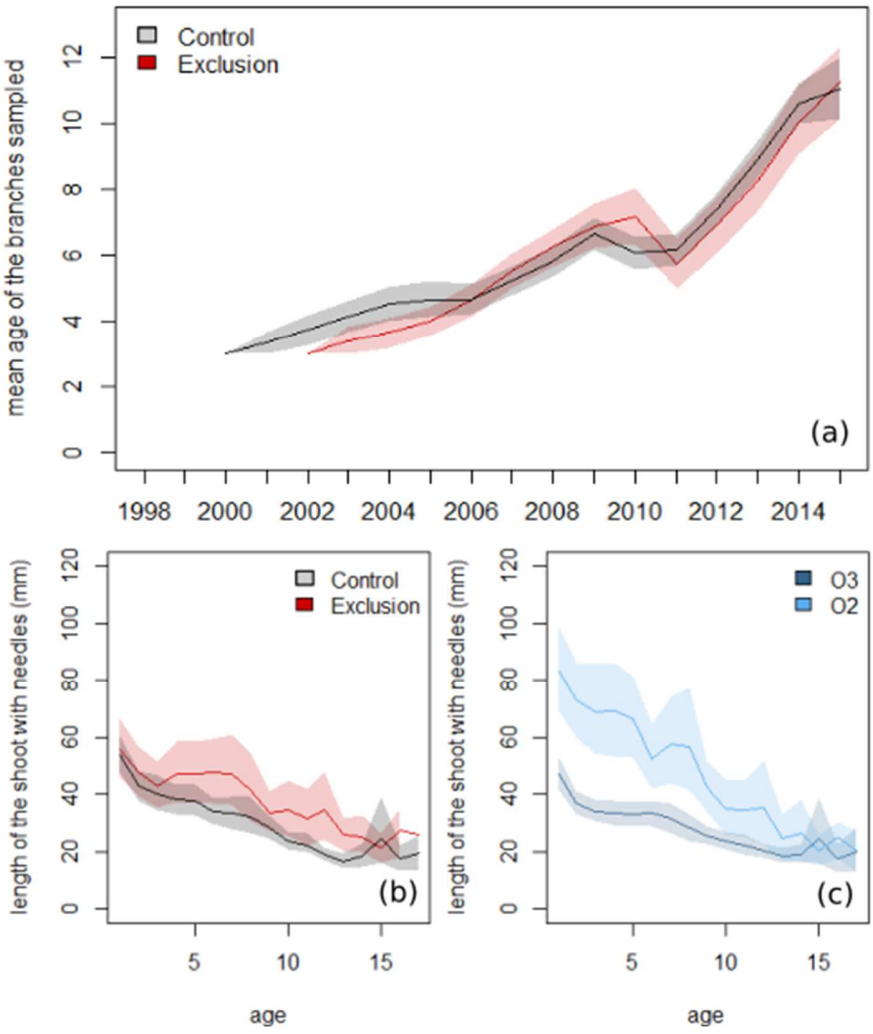

Fig. A2. (a) Mean age of the branches sampled in the control and exclusion plots. (b, c) Effect of branch age on the needle-carrying shoot length of *Pinus halepensis* trees (b) in the control and exclusion plots and (c) in terms of to the architectural order of the branch.

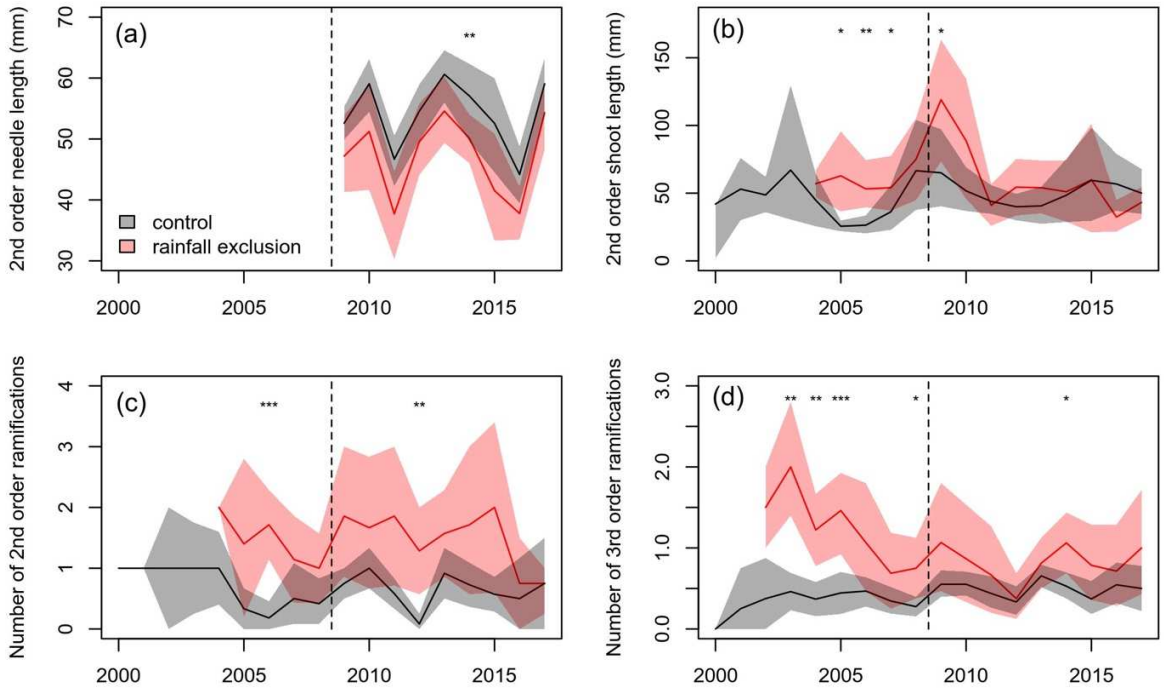

Fig. A3. Time evolutions of (a) the needle length and (b) the shoot length of second order branches and the (c) number of ramifications of second and (d) third order branches of *Pinus halepensis* in the control (black) and rainfall exclusion (red) plots. Significant differences between treatments are displayed for P<0.001 (***), P<0.01 (**) and P<0.05 (*).

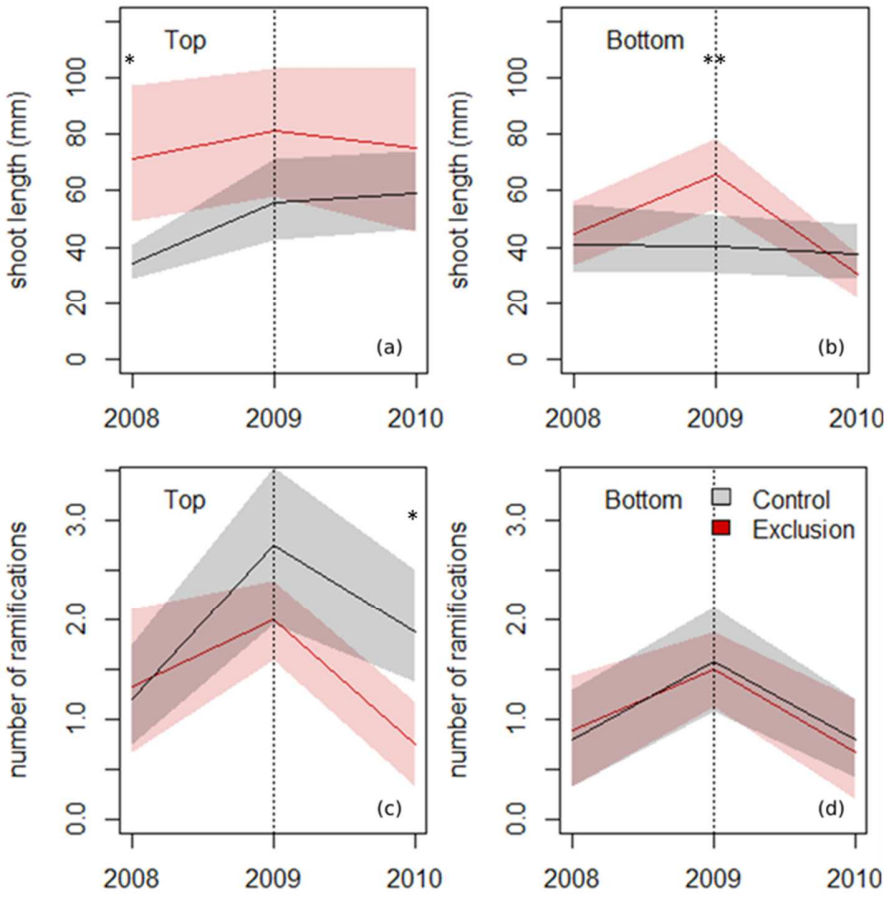

Fig. A4. Time evolutions of (a, b) the shoot length and (c, d) the number of ramifications of *Quercus ilex* branches (a, c) at the top and (b, d) at the bottom of the canopy in the control (black) and rainfall exclusion (red) plots. Significant differences between treatments are displayed for P<0.001 (***), P<0.01 (**) and P<0.05 (*).